RADIATIVE TRANSFER THEORY: FROM MAXWELL'S EQUATIONS TO PRACTICAL APPLICATIONS

MICHAEL I. MISHCHENKO

NASA Goddard Institute for Space Studies, 2880 Broadway, New York, NY 10025, USA

1. Introduction

Since the pioneering papers by Khvolson [1] and Schuster [2], the radiative transfer theory (RTT) has been a basic working tool in astrophysics, atmospheric physics, and remote sensing [3–11], while the radiative transfer equation (RTE) has become a classical equation of mathematical physics [12–15]. However, the RTT has been often criticized for its phenomenological character, lack of solid physical background, and unknown range of applicability [e.g., 16]. The past three decades have demonstrated substantial progress in studies of the statistical wave content of the RTT (e.g., [17–24] and references therein). This research has resulted in a much better understanding of the physical foundation of the RTT and has ultimately made the RTE a corollary of the statistical electromagnetics [25].

The aim of this chapter is to demonstrate how the RTE follows from the Maxwell equations when the latter are applied to the problem of multiple electromagnetic scattering in discrete random media and to discuss how this equation can be solved in practice. The following section contains a brief summary of those principles of classical electromagnetics that form the basis of the theory of single light scattering by a small particle. Section 3 outlines the derivation of the general RTE starting from the vector form of the Foldy-Lax equations for a fixed N-particle system and their far-field version. Based on the assumption that particle positions are completely random, the RTE is derived by applying the Twersky approximation to the coherent electric field and the Twersky and ladder approximations to the coherency dyad of the diffuse field in the limit $N \to \infty$. We then discuss in detail the assumptions leading to the RTE and the physical meaning of the quantities entering this equation. The final section describes a general technique for solving the RTE that allows efficient software implementation and leads to physically based practical applications.

2. Single scattering

Many quantities used in the derivation of the RTE and finally entering it originate in the electromagnetic theory of scattering by a single particle. Therefore, we will introduce in this section the necessary single-scattering concepts and definitions and briefly recapitulate the

B.A. van Tiggelen and S.E. Skipetrov (eds.)
Wave Scattering in Complex Media: From Theory to Applications, 367–414.

results that will be necessary for understanding the material presented in the following sections. A comprehensive treatment of the subject of single scattering, including explicit derivations of all formulas, can be found in [26].

2.1. COHERENCY MATRIX, COHERENCY VECTOR, AND STOKES VECTOR

In order to introduce the basic radiometric and polarimetric characteristics of a transverse electromagnetic wave, we use a local Cartesian coordinate system with origin at the observation point (Fig. 1) and specify the direction of propagation of the wave by a unit vector $\hat{\mathbf{n}} = \{\theta, \varphi\}$, where $\theta \in [0, \pi]$ is the zenith angle and $\varphi \in [0, 2\pi)$ is the azimuth angle measured from the positive *x*-axis in the clockwise direction when looking in the direction of the positive *z*-axis. Because the wave is assumed to be transverse, the electric field at the observation point can be expressed as $\mathbf{E} = \mathbf{E}_\theta + \mathbf{E}_\varphi = E_\theta \hat{\boldsymbol{\theta}} + E_\varphi \hat{\boldsymbol{\varphi}}$, where $\mathbf{E}_\theta$ and $\mathbf{E}_\varphi$ are the θ- and φ-components of the electric field vector.

Consider a time-harmonic plane electromagnetic wave propagating in a homogeneous, linear, isotropic, and nonabsorbing medium with a real electric permittivity ε and a real magnetic susceptibility μ:

$$\mathbf{E}(\mathbf{r}) = \mathbf{E}_0 \exp(\mathrm{i}k\hat{\mathbf{n}} \cdot \mathbf{r}), \qquad \mathbf{E}_0 \cdot \hat{\mathbf{n}} = 0, \tag{1}$$

where the time factor $\exp(-\mathrm{i}\omega t)$ is omitted, $k = \omega\sqrt{\varepsilon\mu}$ is the wave number, and ω is the angular frequency. The 2×2 coherency matrix $\boldsymbol{\rho}$ is defined by

$$\boldsymbol{\rho} = \begin{bmatrix} \rho_{11} & \rho_{12} \\ \rho_{21} & \rho_{22} \end{bmatrix} = \frac{1}{2}\sqrt{\frac{\varepsilon}{\mu}} \begin{bmatrix} E_{0\theta} E_{0\theta}^* & E_{0\theta} E_{0\varphi}^* \\ E_{0\varphi} E_{0\theta}^* & E_{0\varphi} E_{0\varphi}^* \end{bmatrix}, \tag{2}$$

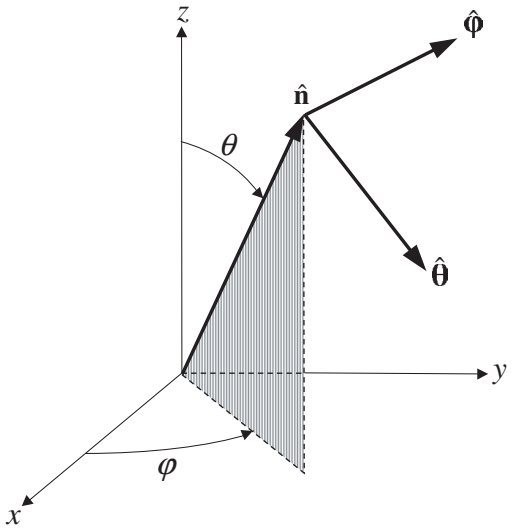

Fig. 1. Local coordinate system used to describe the direction of propagation and the polarization state of a transverse electromagnetic wave.

where the asterisk denotes a complex-conjugate value. The elements of $\boldsymbol{\rho}$ have the dimension of monochromatic energy flux (Wm^{-2}) and can be also grouped into a 4×1 coherency column vector:

$$\mathbf{J}=\begin{bmatrix}\rho_{11}\\ \rho_{12}\\ \rho_{21}\\ \rho_{22}\end{bmatrix}=\frac{1}{2}\sqrt{\frac{\varepsilon}{\mu}}\begin{bmatrix}E_{0\theta}E_{0\theta}^{*}\\ E_{0\theta}E_{0\varphi}^{*}\\ E_{0\varphi}E_{0\theta}^{*}\\ E_{0\varphi}E_{0\varphi}^{*}\end{bmatrix}. \tag{3}$$

The Stokes parameters I, Q, U, and V are then defined as the elements of a 4×1 column Stokes vector $\mathbf{I}$:

$$\mathbf{I}=\mathbf{D}\mathbf{J}=\frac{1}{2}\sqrt{\frac{\varepsilon}{\mu}}\begin{bmatrix}E_{0\theta}E_{0\theta}^{*}+E_{0\varphi}E_{0\varphi}^{*}\\ E_{0\theta}E_{0\theta}^{*}-E_{0\varphi}E_{0\varphi}^{*}\\ -E_{0\theta}E_{0\varphi}^{*}-E_{0\varphi}E_{0\theta}^{*}\\ \mathrm{i}(E_{0\varphi}E_{0\theta}^{*}-E_{0\theta}E_{0\varphi}^{*})\end{bmatrix}=\begin{bmatrix}I\\ Q\\ U\\ V\end{bmatrix}, \tag{4}$$

where

$$\mathbf{D}=\begin{bmatrix}1 & 0 & 0 & 1\\ 1 & 0 & 0 & -1\\ 0 & -1 & -1 & 0\\ 0 & -\mathrm{i} & \mathrm{i} & 0\end{bmatrix}. \tag{5}$$

2.2. VOLUME INTEGRAL EQUATION AND LIPPMANN-SCHWINGER EQUATION

Consider a scattering object that occupies a finite interior region V_{INT} and is surrounded by the infinite exterior region V_{EXT}. The interior region is filled with an isotropic, linear, and possibly inhomogeneous material.

The monochromatic Maxwell curl equations describing the scattering of a time-harmonic electromagnetic field are as follows:

$$\left.\begin{aligned}\nabla\times\mathbf{E}(\mathbf{r})&=\mathrm{i}\omega\mu_1\mathbf{H}(\mathbf{r})\\ \nabla\times\mathbf{H}(\mathbf{r})&=-\mathrm{i}\omega\varepsilon_1\mathbf{E}(\mathbf{r})\end{aligned}\right\}\ \text{for}\ \mathbf{r}\in V_{\mathrm{EXT}}, \tag{6}$$

$$\left.\begin{aligned}\nabla\times\mathbf{E}(\mathbf{r})&=\mathrm{i}\omega\mu_2(\mathbf{r})\mathbf{H}(\mathbf{r})\\ \nabla\times\mathbf{H}(\mathbf{r})&=-\mathrm{i}\omega\varepsilon_2(\mathbf{r})\mathbf{E}(\mathbf{r})\end{aligned}\right\}\ \text{for}\ \mathbf{r}\in V_{\mathrm{INT}}, \tag{7}$$

where subscripts 1 and 2 refer to the exterior and interior regions, respectively. Since the first relations in Eqs. (6) and (7) yield the magnetic field provided that the electric field is known everywhere, we will look for the solution of these equations in terms of only the electric field. Assuming that the host medium and the scattering object are nonmagnetic, i.e., $\mu_2(\mathbf{r})\equiv\mu_1=\mu_0$, where μ_0 is the permeability of a vacuum, and following the approach described in [26], one can reduce Eqs. (6) and (7) to the following volume integral equation:

$$\mathbf{E}(\mathbf{r}) = \mathbf{E}^{\text{inc}}(\mathbf{r}) + k_1^2 \int_{V_{\text{INT}}} \mathrm{d}^3\mathbf{r}'\, \ddot{G}(\mathbf{r},\mathbf{r}') \cdot \mathbf{E}(\mathbf{r}')\,[m^2(\mathbf{r}') - 1], \qquad \mathbf{r} \in \mathbf{R}^3, \tag{8}$$

where $\ddot{G}(\mathbf{r},\mathbf{r}')$ is the free space dyadic Green's function, $m(\mathbf{r}) = k_2(\mathbf{r})/k_1$ is the refractive index of the interior relative to that of the exterior, and $k_1 = \omega\sqrt{\varepsilon_1\,\mu_0}$ and $k_2(\mathbf{r}) = \omega\sqrt{\varepsilon_2(\mathbf{r})\,\mu_0}$ are the wave numbers in the exterior and interior regions, respectively. Alternatively, the scattered field $\mathbf{E}^{\text{sca}}(\mathbf{r}) = \mathbf{E}(\mathbf{r}) - \mathbf{E}^{\text{inc}}(\mathbf{r})$ can be expressed in terms of the incident field by means of the dyad transition operator $\ddot{T}$:

$$\mathbf{E}^{\text{sca}}(\mathbf{r}) = \int_{V_{\text{INT}}} \mathrm{d}^3\mathbf{r}'\, \ddot{G}(\mathbf{r},\mathbf{r}') \cdot \int_{V_{\text{INT}}} \mathrm{d}^3\mathbf{r}''\, \ddot{T}(\mathbf{r}',\mathbf{r}'') \cdot \mathbf{E}^{\text{inc}}(\mathbf{r}''), \qquad \mathbf{r} \in \mathbf{R}^3. \tag{9}$$

Substituting Eq. (9) in Eq. (8) yields the Lippmann-Schwinger equation for $\ddot{T}$:

$$\begin{aligned}\ddot{T}(\mathbf{r},\mathbf{r}') = {} & k_1^2\,[m^2(\mathbf{r}) - 1]\,\delta(\mathbf{r} - \mathbf{r}')\ddot{I} \\ & + k_1^2\,[m^2(\mathbf{r}) - 1] \int_{V_{\text{INT}}} \mathrm{d}^3\mathbf{r}''\, \ddot{G}(\mathbf{r},\mathbf{r}'') \cdot \ddot{T}(\mathbf{r}'',\mathbf{r}'), \qquad \mathbf{r},\mathbf{r}' \in V_{\text{INT}},\end{aligned} \tag{10}$$

where $\ddot{I}$ is the identity dyad.

2.3. FAR-FIELD SCATTERING

We now choose a point *O* at the geometrical center of the scatterer as the common origin of all position vectors (Fig. 2) and make the standard far-field-zone assumptions that $k_1 r \gg 1$ and that *r* is much larger than any linear dimension of the scatterer. Then Eq. (8) becomes

$$\mathbf{E}^{\text{sca}}(\mathbf{r}) \underset{r\to\infty}{=} \frac{\exp(\mathrm{i}k_1 r)}{r} \frac{k_1^2}{4\pi} (\ddot{I} - \hat{\mathbf{r}} \otimes \hat{\mathbf{r}}) \cdot \int_{V_{\text{INT}}} \mathrm{d}^3\mathbf{r}'\,[m^2(\mathbf{r}') - 1]\,\mathbf{E}(\mathbf{r}') \exp(-\mathrm{i}k_1 \hat{\mathbf{r}} \cdot \mathbf{r}'), \tag{11}$$

where $\otimes$ denotes a dyadic product of two vectors and $\hat{\mathbf{r}} = \mathbf{r}/r$ is a unit vector in the direction of $\mathbf{r}$. The factor $\ddot{I} - \hat{\mathbf{r}} \otimes \hat{\mathbf{r}} = \hat{\boldsymbol{\theta}} \otimes \hat{\boldsymbol{\theta}} + \hat{\boldsymbol{\varphi}} \otimes \hat{\boldsymbol{\varphi}}$ ensures that the scattered spherical wave in the far-field zone is transverse so that

$$\mathbf{E}^{\text{sca}}(\mathbf{r}) \underset{r\to\infty}{=} \frac{\exp(\mathrm{i}k_1 r)}{r} \mathbf{E}_1^{\text{sca}}(\hat{\mathbf{r}}), \qquad \hat{\mathbf{r}} \cdot \mathbf{E}_1^{\text{sca}}(\hat{\mathbf{r}}) = 0, \tag{12}$$

where the scattering amplitude $\mathbf{E}_1^{\text{sca}}(\hat{\mathbf{r}})$ is independent of *r* and describes the angular distribution of the scattered radiation.

Assuming that the incident field is a plane electromagnetic wave $\mathbf{E}^{\text{inc}}(\mathbf{r}) = \mathbf{E}_0^{\text{inc}} \exp(\mathrm{i}k_1 \hat{\mathbf{n}}^{\text{inc}} \cdot \mathbf{r})$ yields

$$\mathbf{E}_1^{\text{sca}}(\hat{\mathbf{n}}^{\text{sca}}) = \ddot{A}(\hat{\mathbf{n}}^{\text{sca}}, \hat{\mathbf{n}}^{\text{inc}}) \cdot \mathbf{E}_0^{\text{inc}}, \tag{13}$$

where $\hat{\mathbf{n}}^{\text{sca}} = \hat{\mathbf{r}}$ (Fig. 2). The elements of the so-called scattering dyad $\ddot{A}(\hat{\mathbf{n}}^{\text{sca}}, \hat{\mathbf{n}}^{\text{inc}})$ have the dimension of length.

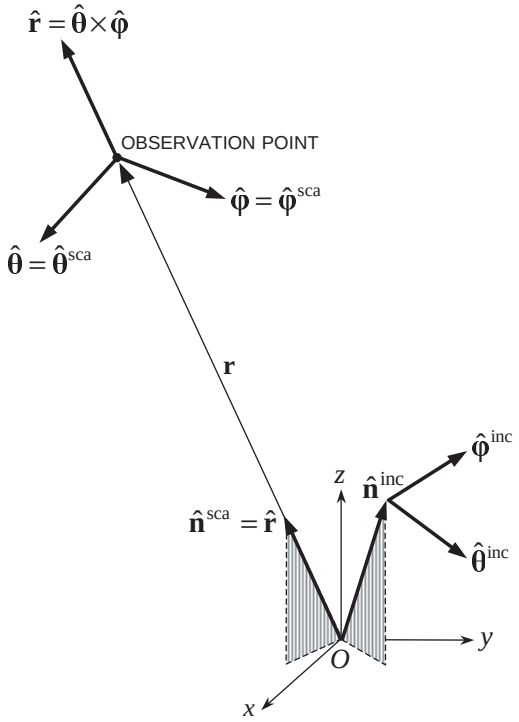

Fig. 2. Scattering in the far-field zone.

It follows from Eq. (12) that $\hat{\mathbf{n}}^{\mathrm{sca}} \cdot \vec{A}(\hat{\mathbf{n}}^{\mathrm{sca}}, \hat{\mathbf{n}}^{\mathrm{inc}}) = 0$. Since $\mathbf{E}_0^{\mathrm{inc}} \cdot \hat{\mathbf{n}}^{\mathrm{inc}} = 0$, the dot product $\vec{A}(\hat{\mathbf{n}}^{\mathrm{sca}}, \hat{\mathbf{n}}^{\mathrm{inc}}) \cdot \hat{\mathbf{n}}^{\mathrm{inc}}$ is not defined by Eq. (13). To complete the definition, we take this product to be zero. As a consequence, only four out of nine components of the scattering dyad are independent. It is therefore convenient to introduce a 2×2 amplitude matrix $\mathbf{S}$, which describes the transformation of the θ- and φ-components of the incident plane wave into the θ- and φ-components of the scattered spherical wave (Fig. 2):

$$\mathbf{E}^{\mathrm{sca}}(r\hat{\mathbf{n}}^{\mathrm{sca}}) \underset{r\to\infty}{=} \frac{\exp(\mathrm{i}k_1 r)}{r} \mathbf{S}(\hat{\mathbf{n}}^{\mathrm{sca}}, \hat{\mathbf{n}}^{\mathrm{inc}}) \mathbf{E}_0^{\mathrm{inc}}, \tag{14}$$

where $\mathbf{E}$ denotes a two-component column formed by the θ- and φ-components of the electric vector. The elements of the amplitude matrix are expressed in terms of the scattering dyad as follows:

$$\begin{aligned} S_{11} &= \hat{\boldsymbol{\theta}}^{\mathrm{sca}} \cdot \vec{A} \cdot \hat{\boldsymbol{\theta}}^{\mathrm{inc}}, \qquad S_{12} = \hat{\boldsymbol{\theta}}^{\mathrm{sca}} \cdot \vec{A} \cdot \hat{\boldsymbol{\varphi}}^{\mathrm{inc}}, \\ S_{21} &= \hat{\boldsymbol{\varphi}}^{\mathrm{sca}} \cdot \vec{A} \cdot \hat{\boldsymbol{\theta}}^{\mathrm{inc}}, \qquad S_{22} = \hat{\boldsymbol{\varphi}}^{\mathrm{sca}} \cdot \vec{A} \cdot \hat{\boldsymbol{\varphi}}^{\mathrm{inc}}. \end{aligned} \tag{15}$$

2.4. PHASE AND EXTINCTION MATRICES

The relationship between the coherency vectors of the incident and scattered light for scattering directions away from the incidence direction ($\hat{\mathbf{r}} \neq \hat{\mathbf{n}}^{\mathrm{inc}}$) in the far-field zone is

described by the 4×4 coherency phase matrix $\mathbf{Z}^J$:

$$\mathbf{J}^{\rm sca}(r\hat{\mathbf{n}}^{\rm sca})=\frac{1}{r^2}\mathbf{Z}^J(\hat{\mathbf{n}}^{\rm sca},\hat{\mathbf{n}}^{\rm inc})\,\mathbf{J}^{\rm inc}, \tag{16}$$

where the coherency vectors of the incident plane wave and the scattered spherical wave are given by

$$\mathbf{J}^{\rm inc}=\frac{1}{2}\sqrt{\frac{\varepsilon_1}{\mu_0}}\begin{bmatrix}E_{0\theta}^{\rm inc}E_{0\theta}^{\rm inc*}\\ E_{0\theta}^{\rm inc}E_{0\varphi}^{\rm inc*}\\ E_{0\varphi}^{\rm inc}E_{0\theta}^{\rm inc*}\\ E_{0\varphi}^{\rm inc}E_{0\varphi}^{\rm inc*}\end{bmatrix},\qquad \mathbf{J}^{\rm sca}(r\hat{\mathbf{n}}^{\rm sca})=\frac{1}{r^2}\frac{1}{2}\sqrt{\frac{\varepsilon_1}{\mu_0}}\begin{bmatrix}E_{1\theta}^{\rm sca}(\hat{\mathbf{n}}^{\rm sca})[E_{1\theta}^{\rm sca}(\hat{\mathbf{n}}^{\rm sca})]^*\\ E_{1\theta}^{\rm sca}(\hat{\mathbf{n}}^{\rm sca})[E_{1\varphi}^{\rm sca}(\hat{\mathbf{n}}^{\rm sca})]^*\\ E_{1\varphi}^{\rm sca}(\hat{\mathbf{n}}^{\rm sca})[E_{1\theta}^{\rm sca}(\hat{\mathbf{n}}^{\rm sca})]^*\\ E_{1\varphi}^{\rm sca}(\hat{\mathbf{n}}^{\rm sca})[E_{1\varphi}^{\rm sca}(\hat{\mathbf{n}}^{\rm sca})]^*\end{bmatrix}, \tag{17}$$

and the elements of $\mathbf{Z}^J(\hat{\mathbf{n}}^{\rm sca},\hat{\mathbf{n}}^{\rm inc})$ are quadratic combinations of the elements of the amplitude matrix $\mathbf{S}(\hat{\mathbf{n}}^{\rm sca},\hat{\mathbf{n}}^{\rm inc})$:

$$\mathbf{Z}^J=\begin{bmatrix}|S_{11}|^2 & S_{11}S_{12}^* & S_{12}S_{11}^* & |S_{12}|^2\\ S_{11}S_{21}^* & S_{11}S_{22}^* & S_{12}S_{21}^* & S_{12}S_{22}^*\\ S_{21}S_{11}^* & S_{21}S_{12}^* & S_{22}S_{11}^* & S_{22}S_{12}^*\\ |S_{21}|^2 & S_{21}S_{22}^* & S_{22}S_{21}^* & |S_{22}|^2\end{bmatrix}. \tag{18}$$

The corresponding Stokes transformation law is

$$\mathbf{I}^{\rm sca}(r\hat{\mathbf{n}}^{\rm sca})=\frac{1}{r^2}\mathbf{Z}(\hat{\mathbf{n}}^{\rm sca},\hat{\mathbf{n}}^{\rm inc})\,\mathbf{I}^{\rm inc}, \tag{19}$$

where $\mathbf{I}^{\rm inc}=\mathbf{D}\mathbf{J}^{\rm inc}$ and $\mathbf{I}^{\rm sca}=\mathbf{D}\mathbf{J}^{\rm sca}$. The explicit expressions for the elements of the Stokes phase matrix $\mathbf{Z}$ follow from Eq. (18) and the obvious formula

$$\mathbf{Z}(\hat{\mathbf{n}}^{\rm sca},\hat{\mathbf{n}}^{\rm inc})=\mathbf{D}\mathbf{Z}^J(\hat{\mathbf{n}}^{\rm sca},\hat{\mathbf{n}}^{\rm inc})\mathbf{D}^{-1}. \tag{20}$$

The coherency vector of the total field for directions $\hat{\mathbf{r}}$ very close to $\hat{\mathbf{n}}^{\rm inc}$ is defined as

$$\mathbf{J}(r\hat{\mathbf{r}})=\frac{1}{2}\sqrt{\frac{\varepsilon_1}{\mu_0}}\begin{bmatrix}E_\theta(r\hat{\mathbf{r}})[E_\theta(r\hat{\mathbf{r}})]^*\\ E_\theta(r\hat{\mathbf{r}})[E_\varphi(r\hat{\mathbf{r}})]^*\\ E_\varphi(r\hat{\mathbf{r}})[E_\theta(r\hat{\mathbf{r}})]^*\\ E_\varphi(r\hat{\mathbf{r}})[E_\varphi(r\hat{\mathbf{r}})]^*\end{bmatrix}, \tag{21}$$

where $\mathbf{E}(r\hat{\mathbf{r}})=\mathbf{E}^{\rm inc}(r\hat{\mathbf{r}})+\mathbf{E}^{\rm sca}(r\hat{\mathbf{r}})$ is the total electric field. Integrating $\mathbf{J}(r\hat{\mathbf{r}})$ over the surface ΔS of a collimated detector facing the incident wave, one can obtain for the total polarized signal:

$$\mathbf{J}(r\hat{\mathbf{n}}^{\rm inc})\Delta S=\mathbf{J}^{\rm inc}\Delta S-\mathbf{K}^J(\hat{\mathbf{n}}^{\rm inc})\mathbf{J}^{\rm inc}+\mathbf{O}(r^{-2}), \tag{22}$$

where the elements of the 4×4 coherency extinction matrix $\mathbf{K}^J(\hat{\mathbf{n}}^{\rm inc})$ are expressed in terms of the elements of the forward-scattering amplitude matrix $\mathbf{S}(\hat{\mathbf{n}}^{\rm inc},\hat{\mathbf{n}}^{\rm inc})$ as follows:

$$\mathbf{K}^J = \frac{\mathrm{i}2\pi}{k_1}\begin{bmatrix} S_{11}^* - S_{11} & S_{12}^* & -S_{12} & 0 \\ S_{21}^* & S_{22}^* - S_{11} & 0 & -S_{12} \\ -S_{21} & 0 & S_{11}^* - S_{22} & S_{12}^* \\ 0 & -S_{21} & S_{21}^* & S_{22}^* - S_{22} \end{bmatrix}. \tag{23}$$

In the Stokes-vector representation,

$$\mathbf{I}(r\hat{\mathbf{n}}^{\mathrm{inc}})\Delta S = \mathbf{I}^{\mathrm{inc}}\Delta S - \mathbf{K}(\hat{\mathbf{n}}^{\mathrm{inc}})\,\mathbf{I}^{\mathrm{inc}} + \mathbf{O}(r^{-2}), \tag{24}$$

where $\mathbf{I}(r\hat{\mathbf{n}}^{\mathrm{inc}}) = \mathbf{D}\mathbf{J}(r\hat{\mathbf{n}}^{\mathrm{inc}})$. Expressions for the elements of the 4×4 Stokes extinction matrix $\mathbf{K}(\hat{\mathbf{n}}^{\mathrm{inc}})$ follow from Eq. (23) and the formula

$$\mathbf{K}(\hat{\mathbf{n}}^{\mathrm{inc}}) = \mathbf{D}\mathbf{K}^J(\hat{\mathbf{n}}^{\mathrm{inc}})\mathbf{D}^{-1}. \tag{25}$$

Equations (22) and (24) represent the most general form of the optical theorem and show that the presence of the scattering particle changes not only the total power of the electromagnetic radiation received by the detector facing the incident wave, but also, perhaps, its state of polarization. The latter phenomenon is called dichroism and results from different attenuation rates for different polarization components of the incident wave.

2.5. OPTICAL CROSS SECTIONS

Important optical characteristics of the scattering object are the total scattering, absorption, and extinction cross sections. The scattering cross section C_{sca} is defined such that the product of C_{sca} and the incident monochromatic energy flux gives the total monochromatic power removed from the incident wave owing to scattering of the incident radiation in all directions. Similarly, the product of the absorption cross section C_{abs} and the incident monochromatic energy flux is equal to the total monochromatic power removed from the incident wave as a result of absorption of light by the object. Finally, the extinction cross section C_{ext} is the sum of the scattering and absorption cross sections and characterizes the total monochromatic power removed from the incident light due to the combined effect of scattering and absorption.

Explicit formulas for the extinction and scattering cross sections are as follows:

$$\begin{aligned} C_{\mathrm{ext}} = \frac{1}{I^{\mathrm{inc}}}[&K_{11}(\hat{\mathbf{n}}^{\mathrm{inc}})\,I^{\mathrm{inc}} + K_{12}(\hat{\mathbf{n}}^{\mathrm{inc}})Q^{\mathrm{inc}} \\ &+ K_{13}(\hat{\mathbf{n}}^{\mathrm{inc}})U^{\mathrm{inc}} + K_{14}(\hat{\mathbf{n}}^{\mathrm{inc}})V^{\mathrm{inc}}], \end{aligned} \tag{26}$$

$$\begin{aligned} C_{\mathrm{sca}} = \frac{1}{I^{\mathrm{inc}}}\int_{4\pi} \mathrm{d}\hat{\mathbf{r}}\,[&Z_{11}(\hat{\mathbf{r}},\hat{\mathbf{n}}^{\mathrm{inc}})I^{\mathrm{inc}} + Z_{12}(\hat{\mathbf{r}},\hat{\mathbf{n}}^{\mathrm{inc}})Q^{\mathrm{inc}} \\ &+ Z_{13}(\hat{\mathbf{r}},\hat{\mathbf{n}}^{\mathrm{inc}})U^{\mathrm{inc}} + Z_{14}(\hat{\mathbf{r}},\hat{\mathbf{n}}^{\mathrm{inc}})V^{\mathrm{inc}}]. \end{aligned} \tag{27}$$

We then have $C_{\mathrm{abs}} = C_{\mathrm{ext}} - C_{\mathrm{sca}} \geq 0$. The single-scattering albedo is defined as the ratio of the scattering and extinction cross sections,

$$\varpi = C_{\text{sca}}/C_{\text{ext}} \le 1, \tag{28}$$

and is equal to unity for nonabsorbing particles.

2.6 SINGLE SCATTERING BY A SMALL COLLECTION OF RANDOMLY POSITIONED PARTICLES

The formalism described above can also be applied to *single scattering* by tenuous particle collections under certain simplifying assumptions. Consider a volume element having a linear dimension l and comprising a number N of randomly positioned particles. We assume that N is sufficiently small and that the mean distance between the particles is large enough that the contribution of light scattered by the particles to the total field exciting each particle is much weaker than the external incident field and can be neglected. We also assume that the positions of the particles are sufficiently random that there are no systematic phase relations between individual waves scattered by different particles. Consider now far-field scattering by the entire volume element by assuming that the observation point is located at a distance much greater than both l and the wavelength of the incident light. It can then be shown [26] that the cumulative optical characteristics of the entire volume element are obtained by incoherently adding the respective optical characteristics of the individual particles:

$$C_{\text{ext}} = \sum_{i=1}^{N} (C_{\text{ext}})_i = N\langle C_{\text{ext}} \rangle, \tag{29}$$

$$C_{\text{sca}} = \sum (C_{\text{sca}})_i = N\langle C_{\text{sca}} \rangle, \tag{30}$$

$$C_{\text{abs}} = \sum (C_{\text{abs}})_i = N\langle C_{\text{abs}} \rangle, \tag{31}$$

$$\mathbf{K} = \sum \mathbf{K}_i = N\langle \mathbf{K} \rangle, \tag{32}$$

$$\mathbf{Z} = \sum \mathbf{Z}_i = N\langle \mathbf{Z} \rangle, \tag{33}$$

where the index i numbers the particles and $\langle C_{\text{ext}} \rangle$, $\langle C_{\text{sca}} \rangle$, $\langle C_{\text{abs}} \rangle$, $\langle \mathbf{K} \rangle$, and $\langle \mathbf{Z} \rangle$ are the average extinction, scattering, and absorption cross sections and the extinction and phase matrices per particle, respectively.

2.7 MACROSCOPICALLY ISOTROPIC AND MIRROR-SYMMETRIC SCATTERING MEDIA

By definition, the phase matrix relates the Stokes parameters of the incident and the scattered beam defined relative to their respective meridional planes. In contrast, the scattering matrix $\mathbf{F}$ relates the Stokes parameters of the incident and the scattered beam defined with respect to the scattering plane, i.e., the plane through the $\hat{\mathbf{n}}^{\text{inc}}$ and $\hat{\mathbf{n}}^{\text{sca}}$. A simple way to introduce the scattering matrix is to direct the z-axis of the laboratory reference frame along the incident beam and superpose the meridional plane with $\varphi = 0$ and the scattering plane:

$$\mathbf{F}(\theta^{\text{sca}}) = \mathbf{Z}(\theta^{\text{sca}}, \varphi^{\text{sca}} = 0;\ \theta^{\text{inc}} = 0, \varphi^{\text{inc}} = 0). \tag{34}$$

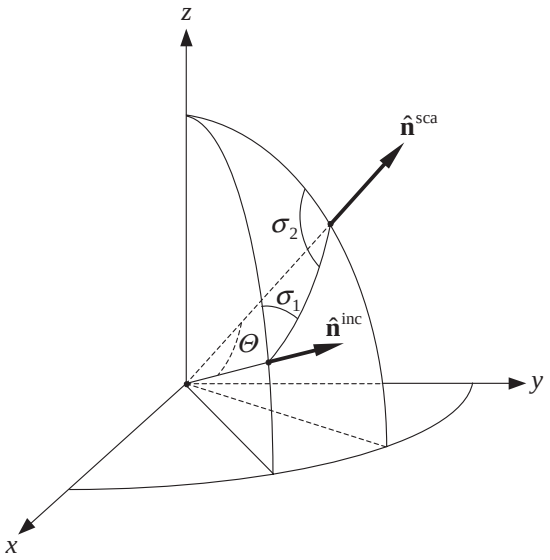

Fig. 3. Relationship between the scattering and phase matrices.

The concept of scattering matrix is especially useful in application to so-called *macroscopically isotropic and mirror-symmetric* scattering media composed of randomly oriented particles with a plane of symmetry and/or equal numbers of randomly oriented particles and their mirror-symmetric counterparts. Indeed, in this case the scattering matrix of a particle collection is independent of incidence direction and orientation of the scattering plane, is functionally dependent only on the scattering angle $\Theta = \arccos(\hat{\mathbf{n}}^{\text{inc}} \cdot \hat{\mathbf{n}}^{\text{sca}})$, and has a simple structure:

$$\mathbf{F}(\Theta) = \begin{bmatrix} F_{11}(\Theta) & F_{12}(\Theta) & 0 & 0 \\ F_{12}(\Theta) & F_{22}(\Theta) & 0 & 0 \\ 0 & 0 & F_{33}(\Theta) & F_{34}(\Theta) \\ 0 & 0 & -F_{34}(\Theta) & F_{44}(\Theta) \end{bmatrix} = N\langle \mathbf{F}(\Theta) \rangle, \tag{35}$$

where $\langle \mathbf{F}(\Theta) \rangle$ is the ensemble-averaged scattering matrix per particle.

Knowledge of the scattering matrix can be used to calculate the Stokes phase matrix for an isotropic and mirror-symmetric scattering medium (Fig. 3). Specifically, to compute the Stokes vector of the scattered beam with respect to its meridional plane, one must:

- calculate the Stokes vector of the incident beam with respect to the scattering plane;
- multiply it by the scattering matrix, thereby obtaining the Stokes vector of the scattered beam with respect to the scattering plane; and finally
- compute the Stokes vector of the scattered beam with respect to its meridional plane.

This procedure yields:

$$\mathbf{Z}(\theta^{\text{sca}}, \varphi^{\text{sca}}; \theta^{\text{inc}}, \varphi^{\text{inc}}) = \mathbf{L}(-\sigma_2)\,\mathbf{F}(\Theta)\,\mathbf{L}(\pi - \sigma_1), \tag{36}$$

where

$$\mathbf{L}(\eta) = \begin{bmatrix} 1 & 0 & 0 & 0 \\ 0 & \cos 2\eta & -\sin 2\eta & 0 \\ 0 & \sin 2\eta & \cos 2\eta & 0 \\ 0 & 0 & 0 & 1 \end{bmatrix} \tag{37}$$

is the Stokes rotation matrix that describes the transformation of the Stokes vector as the reference plane is rotated by an angle η in the clockwise direction when one is looking in the direction of light propagation.

The extinction matrix for an isotropic and mirror-symmetric scattering medium is direction independent and diagonal:

$$\mathbf{K}(\hat{\mathbf{n}}) \equiv \mathbf{K} = N\langle C_{\text{ext}} \rangle \boldsymbol{\Delta} , \tag{38}$$

where $\boldsymbol{\Delta}$ is the 4×4 unit matrix. The average extinction, scattering, and absorption cross sections per particle and the average single-scattering albedo are also independent of the propagation direction of the incident light as well as of its polarization state.

It is convenient in the RTT to use the so-called normalized scattering matrix

$$\widetilde{\mathbf{F}}(\Theta) = \frac{4\pi}{\langle C_{\text{sca}} \rangle} \langle \mathbf{F}(\Theta) \rangle = \begin{bmatrix} a_1(\Theta) & b_1(\Theta) & 0 & 0 \\ b_1(\Theta) & a_2(\Theta) & 0 & 0 \\ 0 & 0 & a_3(\Theta) & b_2(\Theta) \\ 0 & 0 & -b_2(\Theta) & a_4(\Theta) \end{bmatrix} \tag{39}$$

with dimensionless elements. The (1, 1)-element of this matrix, traditionally called the phase function, is normalized to unity according to

$$\tfrac{1}{2} \int_0^\pi d\Theta \sin\Theta \, a_1(\Theta) = 1 . \tag{40}$$

Similarly, the normalized phase matrix can be defined as

$$\widetilde{\mathbf{Z}}(\vartheta^{\text{sca}}, \varphi^{\text{sca}}; \vartheta^{\text{inc}}, \varphi^{\text{inc}}) = \frac{4\pi}{\langle C_{\text{sca}} \rangle} \langle \mathbf{Z}(\vartheta^{\text{sca}}, \varphi^{\text{sca}}; \vartheta^{\text{inc}}, \varphi^{\text{inc}}) \rangle . \tag{41}$$

3. Multiple Scattering

3.1. FOLDY-LAX EQUATIONS

We will now study *multiple scattering* by large particle collections and eventually derive the RTE. We begin by considering electromagnetic scattering by a *fixed* group of N particles collectively occupying the interior region $V_{\text{INT}} = \bigcup_{i=1}^{N} V_i$, where V_i is the volume occupied by the ith particle. Equation (8) now reads

$$\mathbf{E}(\mathbf{r}) = \mathbf{E}^{\text{inc}}(\mathbf{r}) + \int_{\mathbf{R}^3} \mathrm{d}^3\mathbf{r}' U(\mathbf{r}') \, \overleftrightarrow{G}(\mathbf{r}, \mathbf{r}') \cdot \mathbf{E}(\mathbf{r}') , \qquad \mathbf{r} \in \mathbf{R}^3 , \tag{42}$$

where the total potential function $U(\mathbf{r})$ is given by

$$U(\mathbf{r}) = \sum_{i=1}^{N} U_i(\mathbf{r}), \qquad \mathbf{r} \in \mathbf{R}^3, \tag{43}$$

and $U_i(\mathbf{r})$ is the *i*th-particle potential function. The latter is defined by

$$U_i(\mathbf{r}) = \begin{cases} 0, & \mathbf{r} \notin V_i, \\ k_1^2 \, [m_i^2(\mathbf{r}) - 1], & \mathbf{r} \in V_i, \end{cases} \tag{44}$$

where $m_i(\mathbf{r}) = k_{2i}(\mathbf{r})/k_1$ is the relative refractive index of particle *i*. All position vectors originate at the origin *O* of an arbitrarily chosen laboratory coordinate system. It can then be shown [25] that the total electric field everywhere in space can be expressed as

$$\mathbf{E}(\mathbf{r}) = \mathbf{E}^{\mathrm{inc}}(\mathbf{r}) + \sum_{i=1}^{N} \int_{V_i} \mathrm{d}^3\mathbf{r}' \, \ddot{G}(\mathbf{r}, \mathbf{r}') \cdot \int_{V_i} \mathrm{d}^3\mathbf{r}'' \, \ddot{T}_i(\mathbf{r}', \mathbf{r}'') \cdot \mathbf{E}_i(\mathbf{r}''), \quad \mathbf{r} \in \mathbf{R}^3, \tag{45}$$

where the field $\mathbf{E}_i$ exciting particle *i* is given by

$$\mathbf{E}_i(\mathbf{r}) = \mathbf{E}^{\mathrm{inc}}(\mathbf{r}) + \sum_{j(\neq i)=1}^{N} \mathbf{E}_{ij}^{\mathrm{exc}}(\mathbf{r}), \tag{46}$$

and the $\mathbf{E}_{ij}^{\mathrm{exc}}$ are partial exciting fields given by

$$\mathbf{E}_{ij}^{\mathrm{exc}}(\mathbf{r}) = \int_{V_j} \mathrm{d}^3\mathbf{r}' \, \ddot{G}(\mathbf{r}, \mathbf{r}') \cdot \int_{V_j} \mathrm{d}^3\mathbf{r}'' \, \ddot{T}_j(\mathbf{r}', \mathbf{r}'') \cdot \mathbf{E}_j(\mathbf{r}''), \qquad \mathbf{r} \in V_i. \tag{47}$$

The $\ddot{T}_i$ satisfies the Lippmann-Schwinger equation

$$\ddot{T}_i(\mathbf{r}, \mathbf{r}') = U_i(\mathbf{r}) \, \delta(\mathbf{r} - \mathbf{r}') \, \ddot{I} + U_i(\mathbf{r}) \int_{V_i} \mathrm{d}^3\mathbf{r}'' \, \ddot{G}(\mathbf{r}, \mathbf{r}'') \cdot \ddot{T}_i(\mathbf{r}'', \mathbf{r}'), \quad \mathbf{r}, \mathbf{r}' \in V_i, \tag{48}$$

and is the dyad transition operator of particle *i* in the absence of all other particles.

The Foldy-Lax equations (45)–(47) directly follow from Maxwell's equations and describe the process of multiple scattering by a fixed group of *N* particles. Specifically, Eq. (45) decomposes the total field into the vector sum of the incident field and the partial fields generated by each particle in response to the corresponding exciting fields, whereas Eqs. (46) and (47) show that the field exciting each particle consists of the incident field and the fields generated by all other particles.

3.2. FAR-FIELD ZONE APPROXIMATION

Assume now that the distance between any two particles in the group is much greater than the wavelength and much greater than the particle sizes, which means that each particle is located in the far-field zones of all other particles. This assumption allows us to considerably simplify the Foldy-Lax equations. Indeed, the contribution of the *j*th particle to the field exciting the *i*th particle in Eq. (46) can now be represented as a simple outgoing spherical wave centered at the origin of particle *j*:

$$\mathbf{E}_{ij}^{\mathrm{exc}}(\mathbf{r}) \approx G(r_j)\,\mathbf{E}_{1ij}(\hat{\mathbf{r}}_j) \approx \exp(-\mathrm{i}k_1\hat{\mathbf{R}}_{ij}\cdot\mathbf{R}_i)\,\mathbf{E}_{ij}\,\exp(\mathrm{i}k_1\hat{\mathbf{R}}_{ij}\cdot\mathbf{r}), \qquad \mathbf{r}\in V_i, \tag{49}$$

where

$$G(r) = \frac{\exp(\mathrm{i}k_1 r)}{r}, \tag{50}$$

$$\mathbf{E}_{ij} = G(R_{ij})\,\mathbf{E}_{1ij}(\hat{\mathbf{R}}_{ij}), \qquad \mathbf{E}_{ij}\cdot\hat{\mathbf{R}}_{ij} = 0, \tag{51}$$

$\hat{\mathbf{r}}_j = \mathbf{r}_j/r_j$, $\hat{\mathbf{R}}_{ij} = \mathbf{R}_{ij}/R_{ij}$, $r_j = \left|\mathbf{R}_{ij}+\mathbf{r}-\mathbf{R}_i\right| \underset{R_{ij}\to\infty}{=} R_{ij}+\hat{\mathbf{R}}_{ij}\cdot(\mathbf{r}-\mathbf{R}_i)$, and the vectors $\mathbf{r}$, $\mathbf{r}_j$, $\mathbf{R}_i$, $\mathbf{R}_j$, and $\mathbf{R}_{ij}$ are shown in Fig. 4(a). Obviously, $\mathbf{E}_{ij}$ is the partial exciting field at the origin of the *i*th particle caused by the *j*th particle. Thus, Eqs. (46) and (49) show that each particle is excited by the external field and the superposition of *locally* plane waves from all other particles with amplitudes $\exp(-\mathrm{i}k_1\hat{\mathbf{R}}_{ij}\cdot\mathbf{R}_i)\,\mathbf{E}_{ij}$ and propagation

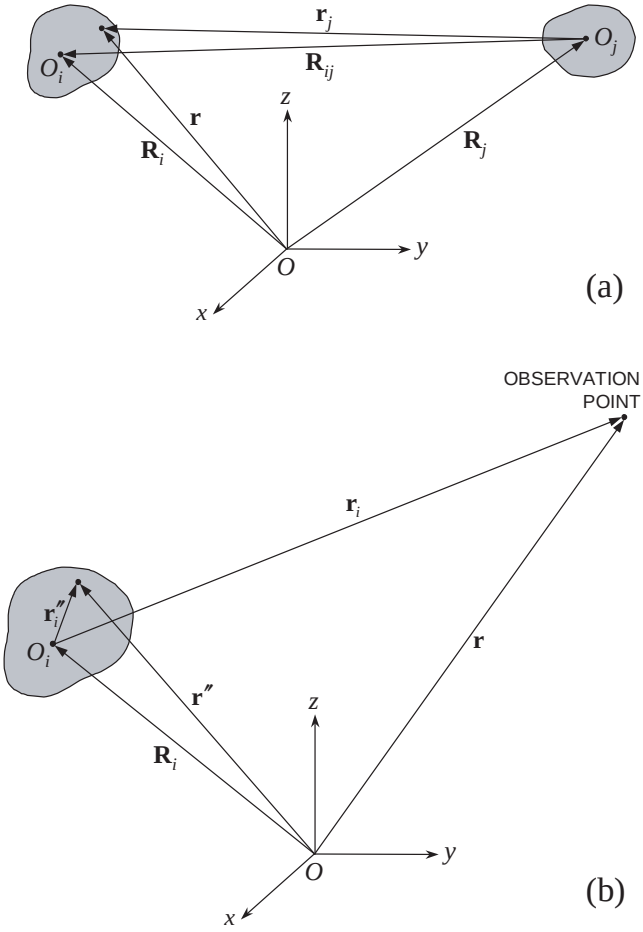

Fig. 4. Scattering by widely separated particles. The local origins O_i and O_j are chosen arbitrarily inside particles *i* and *j*, respectively.

directions $\hat{\mathbf{R}}_{ij}$:

$$\mathbf{E}_i(\mathbf{r}) \approx \mathbf{E}_0^{\text{inc}} \exp(\mathrm{i}k_1\hat{\mathbf{s}}\cdot\mathbf{r}) + \sum_{j(\neq i)=1}^{N} \exp(-\mathrm{i}k_1\hat{\mathbf{R}}_{ij}\cdot\mathbf{R}_i)\,\mathbf{E}_{ij}\exp(\mathrm{i}k_1\hat{\mathbf{R}}_{ij}\cdot\mathbf{r}), \qquad \mathbf{r}\in V_i, \tag{52}$$

where we have assumed that the external incident field is a plane electromagnetic wave $\mathbf{E}^{\text{inc}}(\mathbf{r}) = \mathbf{E}_0^{\text{inc}}\exp(\mathrm{i}k_1\hat{\mathbf{s}}\cdot\mathbf{r})$.

According to Eqs. (12) and (13), the outgoing spherical wave generated by the *j*th particle in response to a plane-wave excitation of the form $\mathbf{E}\exp(\mathrm{i}k_1\hat{\mathbf{n}}\cdot\mathbf{r}_j)$ is given by $G(r_j)\,\ddot{A}_j(\hat{\mathbf{r}}_j,\hat{\mathbf{n}})\cdot\mathbf{E}$, where $\mathbf{r}_j$ originates at O_j and $\ddot{A}_j(\hat{\mathbf{r}}_j,\hat{\mathbf{n}})$ is the *j*th particle scattering dyad centered at O_j . To make use of this fact, we must rewrite Eq. (52) for particle *j* with respect to the *j*th-particle coordinate system centered at O_j , Fig. 4(a). Taking into account that $\mathbf{r} = \mathbf{r}_j + \mathbf{R}_j$ yields

$$\mathbf{E}_j(\mathbf{r}) \approx \mathbf{E}^{\text{inc}}(\mathbf{R}_j)\exp(\mathrm{i}k_1\hat{\mathbf{s}}\cdot\mathbf{r}_j) + \sum_{l(\neq j)=1}^{N} \mathbf{E}_{jl}\exp(\mathrm{i}k_1\hat{\mathbf{R}}_{jl}\cdot\mathbf{r}_j), \qquad \mathbf{r}\in V_j . \tag{53}$$

The electric field at O_i generated in response to this excitation is simply

$$G(R_{ij})\left(\ddot{A}_j(\hat{\mathbf{R}}_{ij},\hat{\mathbf{s}})\cdot\mathbf{E}^{\text{inc}}(\mathbf{R}_j) + \sum_{l(\neq j)=1}^{N}\ddot{A}_j(\hat{\mathbf{R}}_{ij},\hat{\mathbf{R}}_{jl})\cdot\mathbf{E}_{jl}\right). \tag{54}$$

Equating this expression with the right-hand side of Eq. (49) evaluated for $\mathbf{r} = \mathbf{R}_i$ finally yields a system of linear algebraic equations for the partial exciting fields $\mathbf{E}_{ij}$:

$$\mathbf{E}_{ij} = G(R_{ij})\left(\ddot{A}_j(\hat{\mathbf{R}}_{ij},\hat{\mathbf{s}})\cdot\mathbf{E}^{\text{inc}}(\mathbf{R}_j) + \sum_{l(\neq j)=1}^{N}\ddot{A}_j(\hat{\mathbf{R}}_{ij},\hat{\mathbf{R}}_{jl})\cdot\mathbf{E}_{jl}\right), \quad i,j=1,...,N, \quad j\neq i . \tag{55}$$

After the system (55) is solved, one can find the electric field exciting each particle and the total field. Indeed, Eq. (53) gives for a point $\mathbf{r}''\in V_i$:

$$\mathbf{E}_i(\mathbf{r}'') \approx \mathbf{E}^{\text{inc}}(\mathbf{R}_i)\exp(\mathrm{i}k_1\hat{\mathbf{s}}\cdot\mathbf{r}_i'') + \sum_{j(\neq i)=1}^{N}\mathbf{E}_{ij}\exp(\mathrm{i}k_1\hat{\mathbf{R}}_{ij}\cdot\mathbf{r}_i''), \quad \mathbf{r}''\in V_i \tag{56}$$

[see Fig. 4(b)], which is a vector superposition of locally plane waves. Substituting $\mathbf{r}_i'' = 0$ in Eq. (56) yields

$$\mathbf{E}_i(\mathbf{R}_i) = \mathbf{E}^{\text{inc}}(\mathbf{R}_i) + \sum_{j(\neq i)=1}^{N}\mathbf{E}_{ij} . \tag{57}$$

Finally, substituting Eq. (56) in Eq. (45), we derive for the total electric field:

$$\mathbf{E}(\mathbf{r}) = \mathbf{E}^{\text{inc}}(\mathbf{r}) + \sum_{i=1}^{N} G(r_i)\,\ddot{A}_i(\hat{\mathbf{r}}_i,\hat{\mathbf{s}})\cdot\mathbf{E}^{\text{inc}}(\mathbf{R}_i) + \sum_{i=1}^{N} G(r_i)\sum_{j(\neq i)=1}^{N}\ddot{A}_i(\hat{\mathbf{r}}_i,\hat{\mathbf{R}}_{ij})\cdot\mathbf{E}_{ij} , \tag{58}$$

where the observation point **r**, Fig. 4(b), is assumed to be in the far-field zone of any particle forming the group.

3.3. TWERSKY APPROXIMATION

We will now rewrite Eqs. (58) and (55) in a compact form:

$$\mathbf{E} = \mathbf{E}^{\text{inc}} + \sum_{i=1}^{N} \ddot{B}_{ri0} \cdot \mathbf{E}_i^{\text{inc}} + \sum_{i=1}^{N} \sum_{j(\neq i)=1}^{N} \ddot{B}_{rij} \cdot \mathbf{E}_{ij} , \tag{59}$$

$$\mathbf{E}_{ij} = \ddot{B}_{ij0} \cdot \mathbf{E}_j^{\text{inc}} + \sum_{l(\neq j)=1}^{N} \ddot{B}_{ijl} \cdot \mathbf{E}_{jl} , \tag{60}$$

where $\mathbf{E} = \mathbf{E}(\mathbf{r})$, $\mathbf{E}^{\text{inc}} = \mathbf{E}^{\text{inc}}(\mathbf{r})$, $\mathbf{E}_i^{\text{inc}} = \mathbf{E}^{\text{inc}}(\mathbf{R}_i)$,

$$\begin{aligned} \ddot{B}_{ri0} &= G(r_i)\, \ddot{A}_i(\hat{\mathbf{r}}_i, \hat{\mathbf{s}}), \qquad & \ddot{B}_{rij} &= G(r_i)\, \ddot{A}_i(\hat{\mathbf{r}}_i, \hat{\mathbf{R}}_{ij}), \\ \ddot{B}_{ij0} &= G(R_{ij})\, \ddot{A}_j(\hat{\mathbf{R}}_{ij}, \hat{\mathbf{s}}), \qquad & \ddot{B}_{ijl} &= G(R_{ij})\, \ddot{A}_j(\hat{\mathbf{R}}_{ij}, \hat{\mathbf{R}}_{jl}). \end{aligned} \tag{61}$$

Iterating Eq. (60) yields

$$\mathbf{E}_{ij} = \ddot{B}_{ij0} \cdot \mathbf{E}_j^{\text{inc}} + \sum_{\substack{l=1 \\ l\neq j}}^{N} \ddot{B}_{ijl} \cdot \ddot{B}_{jl0} \cdot \mathbf{E}_l^{\text{inc}} + \sum_{\substack{l=1 \\ l\neq j}}^{N} \sum_{\substack{m=1 \\ m\neq l}}^{N} \ddot{B}_{ijl} \cdot \ddot{B}_{jlm} \cdot \ddot{B}_{lm0} \cdot \mathbf{E}_m^{\text{inc}} + \cdots , \tag{62}$$

whereas substituting Eq. (62) in Eq. (59) gives an order-of-scattering expansion of the total electric field:

$$\begin{aligned} \mathbf{E} = \mathbf{E}^{\text{inc}} &+ \sum_{i=1}^{N} \ddot{B}_{ri0} \cdot \mathbf{E}_i^{\text{inc}} + \sum_{i=1}^{N} \sum_{\substack{j=1 \\ j\neq i}}^{N} \ddot{B}_{rij} \cdot \ddot{B}_{ij0} \cdot \mathbf{E}_j^{\text{inc}} \\ &+ \sum_{i=1}^{N} \sum_{\substack{j=1 \\ j\neq i}}^{N} \sum_{\substack{l=1 \\ l\neq j}}^{N} \ddot{B}_{rij} \cdot \ddot{B}_{ijl} \cdot \ddot{B}_{jl0} \cdot \mathbf{E}_l^{\text{inc}} \\ &+ \sum_{i=1}^{N} \sum_{\substack{j=1 \\ j\neq i}}^{N} \sum_{\substack{l=1 \\ l\neq j}}^{N} \sum_{\substack{m=1 \\ m\neq l}}^{N} \ddot{B}_{rij} \cdot \ddot{B}_{ijl} \cdot \ddot{B}_{jlm} \cdot \ddot{B}_{lm0} \cdot \mathbf{E}_m^{\text{inc}} + \cdots . \end{aligned} \tag{63}$$

The terms with $j = i$ and $l = j$ in the triple summation on the right-hand side of Eq. (63) are excluded, but the terms with $l = i$ are not. Therefore, we can decompose this summation as follows:

$$\sum_{i=1}^{N} \sum_{\substack{j=1 \\ j\neq i}}^{N} \sum_{\substack{l=1 \\ l\neq i \\ l\neq j}}^{N} \ddot{B}_{rij} \cdot \ddot{B}_{ijl} \cdot \ddot{B}_{jl0} \cdot \mathbf{E}_l^{\text{inc}} + \sum_{i=1}^{N} \sum_{\substack{j=1 \\ j\neq i}}^{N} \ddot{B}_{rij} \cdot \ddot{B}_{iji} \cdot \ddot{B}_{ji0} \cdot \mathbf{E}_i^{\text{inc}} . \tag{64}$$

Higher-order summations in Eq. (63) can be decomposed similarly. Hence, the total field at an observation point **r** consists of the incident field and single- and multiple-scattering

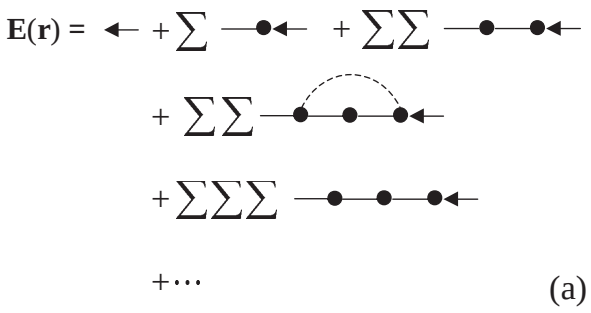

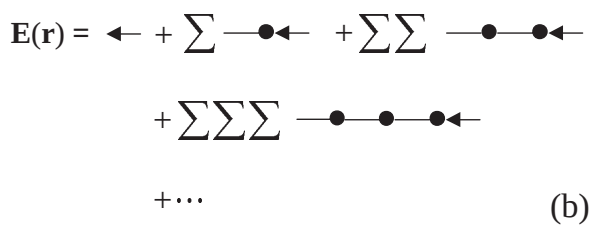

Fig. 5. Diagrammatic representations of (a) Eq. (63) and (b) Eq. (65).

contributions that can be divided into two groups. The first one includes all the terms that correspond to self-avoiding scattering paths, whereas the second group includes all the terms corresponding to the paths that go through a scatterer more than once. The so-called Twersky approximation [27] neglects the terms belonging to the second group and retains only the terms from the first group:

$$\mathbf{E} \approx \mathbf{E}^{\rm inc} + \sum_{i=1}^{N} \vec{\vec{B}}_{ri0} \cdot \mathbf{E}_i^{\rm inc} + \sum_{i=1}^{N} \sum_{\substack{j=1 \\ j\neq i}}^{N} \vec{\vec{B}}_{rij} \cdot \vec{\vec{B}}_{ij0} \cdot \mathbf{E}_j^{\rm inc} + \sum_{i=1}^{N} \sum_{\substack{j=1 \\ j\neq i}}^{N} \sum_{\substack{l=1 \\ l\neq i \\ l\neq j}}^{N} \vec{\vec{B}}_{rij} \cdot \vec{\vec{B}}_{ijl} \cdot \vec{\vec{B}}_{jl0} \cdot \mathbf{E}_l^{\rm inc}$$

$$+ \sum_{i=1}^{N} \sum_{\substack{j=1 \\ j\neq i}}^{N} \sum_{\substack{l=1 \\ l\neq i \\ l\neq j}}^{N} \sum_{\substack{m=1 \\ m\neq i \\ m\neq j \\ m\neq l}}^{N} \vec{\vec{B}}_{rij} \cdot \vec{\vec{B}}_{ijl} \cdot \vec{\vec{B}}_{jlm} \cdot \vec{\vec{B}}_{lm0} \cdot \mathbf{E}_m^{\rm inc} + \cdots . \qquad (65)$$

It is straightforward to show that the Twersky approximation includes the majority of multiple-scattering paths and thus can be expected to yield rather accurate results provided that the number of particles is sufficiently large.

Panel (a) of Fig. 5 visualizes the full expansion (63), whereas panel (b) illustrates the Trwersky approximation (65). The symbol ◄— represents the incident field, the symbol —● denotes multiplying a field by a $\vec{\vec{B}}$ dyad, and the dashed connector indicates that two scattering events involve the same particle.

3.4. COHERENT FIELD

Let us now consider electromagnetic scattering by a large group of N arbitrarily oriented

particles randomly distributed throughout a volume V. The particle ensemble is characterized by a probability density function $p(\mathbf{R}_1,\xi_1;...;\mathbf{R}_i,\xi_i;...;\mathbf{R}_N,\xi_N)$ such that the probability of finding the first particle in the volume element $\mathrm{d}^3\mathbf{R}_1$ centered at $\mathbf{R}_1$ and with its state in the region $\mathrm{d}\xi_1$ centered at ξ_1, …, the ith particle in the volume element $\mathrm{d}^3\mathbf{R}_i$ centered at $\mathbf{R}_i$ and with its state in the region $\mathrm{d}\xi_i$ centered at ξ_i, …, and the Nth particle in the volume element $\mathrm{d}^3\mathbf{R}_N$ centered at $\mathbf{R}_N$ and with its state in the region $\mathrm{d}\xi_N$ centered at ξ_N is given by $p(\mathbf{R}_1,\xi_1;...;\mathbf{R}_N,\xi_N)\prod_{i=1}^{N}\mathrm{d}^3\mathbf{R}_i\,\mathrm{d}\xi_i$. The state of a particle can collectively indicate its size, refractive index, shape, orientation, etc. The statistical average of a random function f depending on all N particles is given by

$$\langle f\rangle = \int f(\mathbf{R}_1,\xi_1;...;\mathbf{R}_N,\xi_N)\,p(\mathbf{R}_1,\xi_1;...;\mathbf{R}_N,\xi_N)\prod_{i=1}^{N}\mathrm{d}^3\mathbf{R}_i\mathrm{d}\xi_i\ . \tag{66}$$

If the position and state of each particle are independent of those of all other particles then

$$p(\mathbf{R}_1,\xi_1;...;\mathbf{R}_N,\xi_N) = \prod_{i=1}^{N} p_i(\mathbf{R}_i,\xi_i)\ . \tag{67}$$

This is a good approximation when particles are sparsely distributed so that the finite size of the particles can be neglected. In this case the effect of size appears only in the particle scattering characteristics. If, furthermore, the state of each particle is independent of its position then

$$p_i(\mathbf{R}_i,\xi_i) = p_{\mathbf{R}i}(\mathbf{R}_i)\,p_{\xi i}(\xi_i)\ . \tag{68}$$

Finally, assuming that all particles have the same statistical characteristics, we have

$$p_i(\mathbf{R}_i,\xi_i) \equiv p(\mathbf{R}_i,\xi_i) = p_{\mathbf{R}}(\mathbf{R}_i)\,p_{\xi}(\xi_i)\ . \tag{69}$$

Obviously,

$$p_{\mathbf{R}}(\mathbf{R}) = n_0(\mathbf{R})/N\ . \tag{70}$$

If the spatial distribution of the N particles throughout the volume V is statistically uniform then

$$n_0(\mathbf{R}) \equiv n_0 = N/V\ , \qquad p_{\mathbf{R}}(\mathbf{R}) = 1/V\ . \tag{71}$$

The electric field $\mathbf{E}(\mathbf{r})$ at a point $\mathbf{r}$ in the scattering medium is a random function of $\mathbf{r}$ and of the coordinates and states of the particles and can be decomposed into the average (coherent) field $\mathbf{E}_{\mathrm{c}}(\mathbf{r})$ and the fluctuating field $\mathbf{E}_{\mathrm{f}}(\mathbf{r})$:

$$\mathbf{E}(\mathbf{r}) = \mathbf{E}_{\mathrm{c}}(\mathbf{r}) + \mathbf{E}_{\mathrm{f}}(\mathbf{r})\ , \qquad \mathbf{E}_{\mathrm{c}}(\mathbf{r}) = \left\langle \mathbf{E}(\mathbf{r})\right\rangle\ , \qquad \left\langle \mathbf{E}_{\mathrm{f}}(\mathbf{r})\right\rangle = 0\ . \tag{72}$$

Assuming that the particles are sparsely distributed and have the same statistical characteristics, we have from Eqs. (65), (67), and (69):

$$\mathbf{E}_{\rm c} = \mathbf{E}^{\rm inc} + \sum_{i=1}^{N} \int \left\langle \ddot{A}(\hat{\mathbf{r}}_i, \hat{\mathbf{s}}) \right\rangle \cdot \mathbf{E}_i^{\rm inc} G(r_i)\, p_{\mathbf{R}}(\mathbf{R}_i)\, {\rm d}^3\mathbf{R}_i$$
$$+ \sum_{i=1}^{N} \sum_{\substack{j=1 \\ j\neq i}}^{N} \int \left\langle \ddot{A}(\hat{\mathbf{r}}_i, \hat{\mathbf{R}}_{ij}) \right\rangle \cdot \left\langle \ddot{A}(\hat{\mathbf{R}}_{ij}, \hat{\mathbf{s}}) \right\rangle \cdot \mathbf{E}_j^{\rm inc} G(r_i) G(R_{ij})$$
$$\times p_{\mathbf{R}}(\mathbf{R}_i)\, p_{\mathbf{R}}(\mathbf{R}_j)\, {\rm d}^3\mathbf{R}_i {\rm d}^3\mathbf{R}_j + \cdots, \tag{73}$$

where $\langle \ddot{A}(\hat{\mathbf{m}}, \hat{\mathbf{n}}) \rangle$ is the average of the scattering dyad over the particle states. Finally, recalling Eq. (70), we obtain in the limit $N \to \infty$:

$$\mathbf{E}_{\rm c} \underset{N\to\infty}{=} \mathbf{E}^{\rm inc} + \int \left\langle \ddot{A}(\hat{\mathbf{r}}_i, \hat{\mathbf{s}}) \right\rangle \cdot \mathbf{E}_i^{\rm inc} G(r_i) n_0(\mathbf{R}_i)\, {\rm d}^3\mathbf{R}_i$$
$$+ \int \left\langle \ddot{A}(\hat{\mathbf{r}}_i, \hat{\mathbf{R}}_{ij}) \right\rangle \cdot \left\langle \ddot{A}(\hat{\mathbf{R}}_{ij}, \hat{\mathbf{s}}) \right\rangle \cdot \mathbf{E}_j^{\rm inc} G(r_i) G(R_{ij})\; n_0(\mathbf{R}_i) n_0(\mathbf{R}_j)\, {\rm d}^3\mathbf{R}_i\, {\rm d}^3\mathbf{R}_j + \cdots, \tag{74}$$

where we have replaced all factors $(N-n)!/N!$ by N^n. This is the general vector form of the expansion derived by Twersky [27] for scalar waves.

Assume now that the particles are distributed uniformly throughout the volume so that $n_0(\mathbf{R}) \equiv n_0$ and that the scattering medium has a concave boundary. The latter assumption ensures that all points of a straight line connecting any two points of the medium lie inside the medium. It is convenient to introduce an *s*-axis parallel to the incidence direction and going through the observation point (Fig. 6). This axis enters the volume *V* at the point *A* such that $s(A) = 0$ and exits it at the point *B*. One can then use the asymptotic expansion of a plane wave in spherical waves [28],

$$\exp({\rm i}k_1 \hat{\mathbf{s}} \cdot \mathbf{R}_i') \underset{k_1 R_i' \to \infty}{=} \frac{{\rm i}2\pi}{k_1 R_i'} [\delta(\hat{\mathbf{s}} + \hat{\mathbf{R}}_i') \exp(-{\rm i}k_1 R_i') - \delta(\hat{\mathbf{s}} - \hat{\mathbf{R}}_i') \exp({\rm i}k_1 R_i')],$$

and assume that the observation point is in the far-field zone of any particle to derive [25]:

$$\mathbf{E}_{\rm c}(\mathbf{r}) = \exp\left[{\rm i}2\pi n_0 k_1^{-1} s(\mathbf{r}) \langle \ddot{A}(\hat{\mathbf{s}}, \hat{\mathbf{s}}) \rangle\right] \cdot \mathbf{E}^{\rm inc}(\mathbf{r})\,. \tag{75}$$

Since $\mathbf{r} = \mathbf{r}_A + s(\mathbf{r})\hat{\mathbf{s}}$, we have

$$\mathbf{E}_{\rm c}(\mathbf{r}) = \exp[{\rm i}\ddot{\kappa}(\hat{\mathbf{s}}) s(\mathbf{r})] \cdot \mathbf{E}^{\rm inc}(\mathbf{r}_A) = \ddot{\eta}[\hat{\mathbf{s}}, s(\mathbf{r})] \cdot \mathbf{E}^{\rm inc}(\mathbf{r}_A), \tag{76}$$

where

$$\ddot{\kappa}(\hat{\mathbf{s}}) = k_1 \ddot{I} + \frac{2\pi n_0}{k_1} \left\langle \ddot{A}(\hat{\mathbf{s}}, \hat{\mathbf{s}}) \right\rangle \tag{77}$$

is the dyadic propagation constant for the propagation direction $\hat{\mathbf{s}}$ and

$$\ddot{\eta}(\hat{\mathbf{s}}, s) = \exp[{\rm i}\ddot{\kappa}(\hat{\mathbf{s}}) s] \tag{78}$$

is the coherent transmission dyad. This is the general vector form of the Foldy

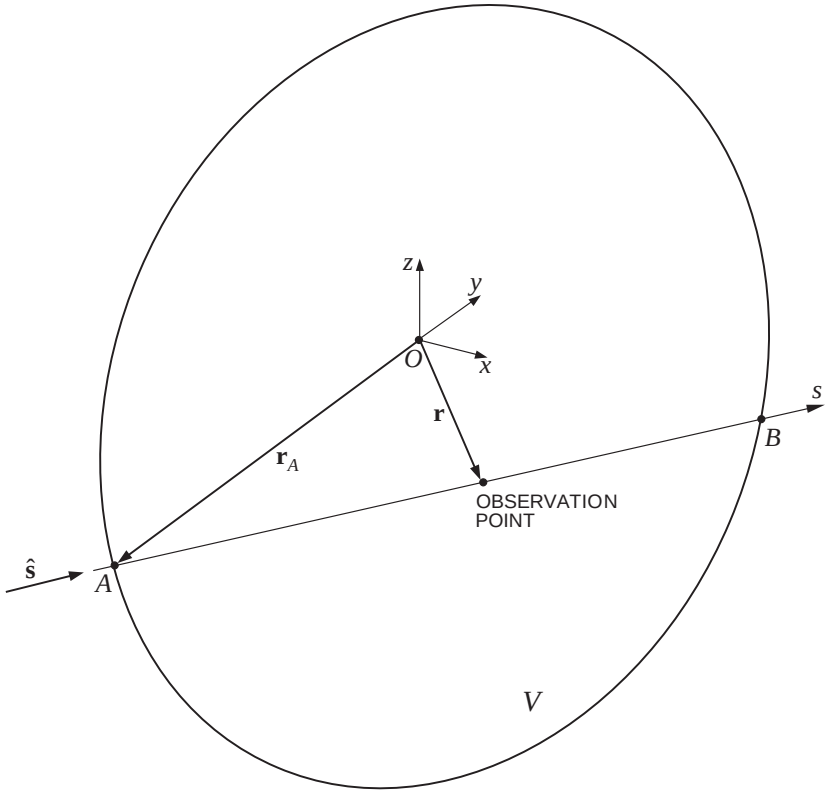

Fig. 6. Scattering volume

approximation for the coherent field. Another form of Eq. (76) is

$$\frac{\mathrm{d}\mathbf{E}_{\mathrm{c}}(\mathbf{r})}{\mathrm{d}s} = \mathrm{i}\vec{\kappa}(\hat{\mathbf{s}})\cdot\mathbf{E}_{\mathrm{c}}(\mathbf{r})\,. \tag{79}$$

The coherent field also satisfies the vector Helmholtz equation

$$\nabla^2\mathbf{E}_{\mathrm{c}}(\mathbf{r}) + k_1^2\vec{\varepsilon}(\hat{\mathbf{s}})\cdot\mathbf{E}_{\mathrm{c}}(\mathbf{r}) = 0\,, \tag{80}$$

where $\vec{\varepsilon}(\hat{\mathbf{s}}) = \vec{I} + 4\pi n_0 k_1^{-2}\left\langle \vec{A}(\hat{\mathbf{s}},\hat{\mathbf{s}})\right\rangle$ is the effective dyadic dielectric constant.

These results have several important implications. First, they show that the coherent field is a wave propagating in the direction of the incident field $\hat{\mathbf{s}}$. Second, since the products $\left\langle \vec{A}(\hat{\mathbf{s}},\hat{\mathbf{s}})\right\rangle\cdot\mathbf{E}_0^{\mathrm{inc}}$, $\left\langle \vec{A}(\hat{\mathbf{s}},\hat{\mathbf{s}})\right\rangle\cdot\left\langle \vec{A}(\hat{\mathbf{s}},\hat{\mathbf{s}})\right\rangle\cdot\mathbf{E}_0^{\mathrm{inc}}$, etc. always give electric vectors normal to $\hat{\mathbf{s}}$, the coherent wave is transverse: $\mathbf{E}_{\mathrm{c}}(\mathbf{r})\cdot\hat{\mathbf{s}} = 0$. Third, Eq. (77) generalizes the optical theorem to the case of many scatterers by expressing the dyadic propagation constant in terms of the forward-scattering amplitude matrix averaged over the particle ensemble.

We can now make use of the transverse character of the coherent wave to rewrite the above equations in a simpler matrix form. As usual, we characterize the propagation direction $\hat{\mathbf{s}}$ at the observation point $\mathbf{r}$ using the corresponding zenith and azimuth angles

in the local coordinate system centered at the observation point and having the same spatial orientation as the laboratory coordinate system $\{x, y, z\}$ (Fig. 6). Then the coherent field can be written as $\mathbf{E}_{\mathrm{c}}(\mathbf{r}) = E_{\mathrm{c}\theta}(\mathbf{r})\hat{\boldsymbol{\theta}} + E_{\mathrm{c}\varphi}(\mathbf{r})\hat{\boldsymbol{\varphi}}$. Denoting, as always, the two-component electric column-vector of the coherent field by $\mathbf{E}_{\mathrm{c}}(\mathbf{r})$, we have

$$\frac{\mathrm{d}\mathbf{E}_{\mathrm{c}}(\mathbf{r})}{\mathrm{d}s} = \mathrm{i}\mathbf{k}(\hat{\mathbf{s}})\mathbf{E}_{\mathrm{c}}(\mathbf{r}), \tag{81}$$

where $\mathbf{k}(\hat{\mathbf{s}})$ is the 2×2 matrix propagation constant with elements

$$\begin{aligned} k_{11}(\hat{\mathbf{s}}) &= \hat{\boldsymbol{\theta}}(\hat{\mathbf{s}})\cdot\vec{\kappa}(\hat{\mathbf{s}})\cdot\hat{\boldsymbol{\theta}}(\hat{\mathbf{s}}), \qquad k_{12}(\hat{\mathbf{s}}) = \hat{\boldsymbol{\theta}}(\hat{\mathbf{s}})\cdot\vec{\kappa}(\hat{\mathbf{s}})\cdot\hat{\boldsymbol{\varphi}}(\hat{\mathbf{s}}), \\ k_{21}(\hat{\mathbf{s}}) &= \hat{\boldsymbol{\varphi}}(\hat{\mathbf{s}})\cdot\vec{\kappa}(\hat{\mathbf{s}})\cdot\hat{\boldsymbol{\theta}}(\hat{\mathbf{s}}), \qquad k_{22}(\hat{\mathbf{s}}) = \hat{\boldsymbol{\varphi}}(\hat{\mathbf{s}})\cdot\vec{\kappa}(\hat{\mathbf{s}})\cdot\hat{\boldsymbol{\varphi}}(\hat{\mathbf{s}}). \end{aligned} \tag{82}$$

Obviously,

$$\mathbf{k}(\hat{\mathbf{s}}) = k_1\mathrm{diag}[1,1] + \frac{2\pi n_0}{k_1}\left\langle \mathbf{S}(\hat{\mathbf{s}},\hat{\mathbf{s}})\right\rangle, \tag{83}$$

where $\langle \mathbf{S}(\hat{\mathbf{s}},\hat{\mathbf{s}})\rangle$ is the forward-scattering amplitude matrix averaged over the particle states.

It is not surprising that the propagation of the coherent field is controlled by the forward-scattering amplitude matrix. Indeed, the fluctuating component of the total field is the sum of the partial fields generated by different particles. Random movements of the particles involve large phase shifts in the partial fields and cause the fluctuating field to vanish when it is averaged over particle positions. The exact forward-scattering direction is different because in any plane parallel to the incident wave-front, the phase of the partial wave forward-scattered by a particle in response to the incident wave does not depend on the particle position. Therefore, the interference of the incident wave and the forward-scattered partial wave is always the same irrespective of the particle position, and the result of the interference does not vanish upon averaging over all particle positions.

3.5. TRANSFER EQUATION FOR THE COHERENT FIELD

We will now switch to quantities that have the dimension of monochromatic energy flux and can thus be measured by an optical device. We first define the coherency column vector of the coherent field according to

$$\mathbf{J}_{\mathrm{c}} = \frac{1}{2}\sqrt{\frac{\varepsilon_1}{\mu_0}}\begin{bmatrix} E_{\mathrm{c}\theta}E_{\mathrm{c}\theta}^* \\ E_{\mathrm{c}\theta}E_{\mathrm{c}\varphi}^* \\ E_{\mathrm{c}\varphi}E_{\mathrm{c}\theta}^* \\ E_{\mathrm{c}\varphi}E_{\mathrm{c}\varphi}^* \end{bmatrix} \tag{84}$$

and derive from Eqs. (81) and (83) the following transfer equation:

$$\frac{\mathrm{d}\mathbf{J}_{\mathrm{c}}(\mathbf{r})}{\mathrm{d}s} = -n_0\left\langle \mathbf{K}^J(\hat{\mathbf{s}})\right\rangle\mathbf{J}_{\mathrm{c}}(\mathbf{r}), \tag{85}$$

where $\mathbf{K}^J$ is the coherency extinction matrix given by Eq. (23). The Stokes-vector

representation of this equation is obtained using the definition $\mathbf{I}_{\rm c} = \mathbf{D}\mathbf{J}_{\rm c}$ and Eq. (25):

$$\frac{{\rm d}\mathbf{I}_{\rm c}(\mathbf{r})}{{\rm d}s} = -n_0 \left\langle \mathbf{K}(\hat{\mathbf{s}}) \right\rangle \mathbf{I}_{\rm c}(\mathbf{r}) , \tag{86}$$

where $\mathbf{K}$ is the Stokes extinction matrix. Both $\mathbf{J}_{\rm c}$ and $\mathbf{I}_{\rm c}$ have the dimension of monochromatic energy flux. The formal solution of Eq. (86) can be written in the form

$$\mathbf{I}_{\rm c}(\mathbf{r}) = \mathbf{H}[\hat{\mathbf{s}}, s(\mathbf{r})] \mathbf{I}_{\rm c}(\mathbf{r}_A) , \tag{87}$$

where

$$\mathbf{H}(\hat{\mathbf{s}}, s) = \exp\left\{ - n_0 \left\langle \mathbf{K}(\hat{\mathbf{s}}) \right\rangle s \right\} \tag{88}$$

is the coherent transmission Stokes matrix.

The interpretation of Eq. (87) is most obvious when the average extinction matrix is given by Eq. (38):

$$\mathbf{I}_{\rm c}(\mathbf{r}) = \exp[-n_0 \langle C_{\rm ext} \rangle s(\mathbf{r})\rangle] \mathbf{I}_{\rm c}(\mathbf{r}_A) = \exp[-\alpha_{\rm ext} s(\mathbf{r})] \mathbf{I}_{\rm c}(\mathbf{r}_A) , \tag{89}$$

which means that the Stokes parameters of the coherent wave are exponentially attenuated as the wave travels through the discrete random medium. The attenuation rates for all four Stokes parameters are the same, which means that the polarization state of the wave does not change. Equation (89) is the standard Beer's law, in which $\alpha_{\rm ext}$ is the extinction coefficient. The attenuation is a combined result of scattering of the coherent field by particles in all directions and, possibly, absorption inside the particles and is an inalienable property of all scattering media, even those composed of nonabsorbing particles with $\langle C_{\rm abs} \rangle = 0$. In general, the extinction matrix is not diagonal and can explicitly depend on the propagation direction. This occurs, for example, when the scattering medium is composed of non-randomly oriented nonspherical particles. Then the coherent transmission matrix $\mathbf{H}$ in Eq. (87) can also have non-zero off-diagonal elements and cause a change in the polarization state of the coherent wave as it propagates through the medium.

3.6. DYADIC CORRELATION FUNCTION

An important statistical characteristic of the multiple-scattering process is the so-called dyadic correlation function defined as the ensemble average of the dyadic product $\mathbf{E}(\mathbf{r}) \otimes \mathbf{E}^*(\mathbf{r}')$. Obviously, the dyadic correlation function has the dimension of monochromatic energy flux. Recalling the Twersky approximation (65) and Fig. 5(b), we conclude that the dyadic correlation function can be represented diagrammatically by Fig. 7. To classify different terms entering the expanded expression inside the angular brackets on the right-hand side of this equation, we will use the notation illustrated in Fig. 8(a). In this particular case, the upper and the lower scattering paths go through different particles. However, the two paths can involve one or more common particles, as shown in panels (b)–(d) by using the dashed connectors. Furthermore, if the number of common particles is two or more, they can enter the upper and lower paths in the same order, as in panel (c), or in reverse order, as in panel (d). Panel (e) is a mixed diagram in which two common particles appear in the same order and two other common particles appear in reverse order.

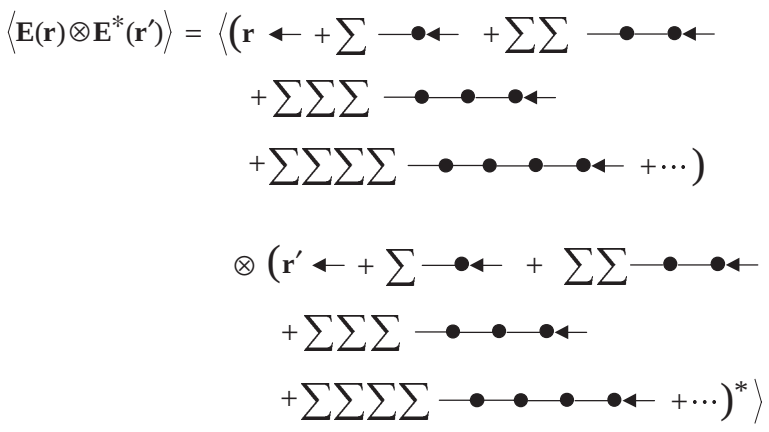

Fig. 7. The Twersky representation of the dyadic correlation function.

According to the Twersky approximation, no particle can be the origin of more than one connector.

To simplify the problem, we will neglect all diagrams with crossing connectors and will take into account only the diagrams with vertical or no connectors. This approximation will allow us to sum and average large groups of diagrams independently and eventually derive the radiative transfer equation.

We begin with diagrams that have no connectors. Since these diagrams do not involve common particles, the ensemble averaging of the upper and lower paths can be performed independently. Consider first the sum of the diagrams shown in Fig. 9(a), in which the Σ

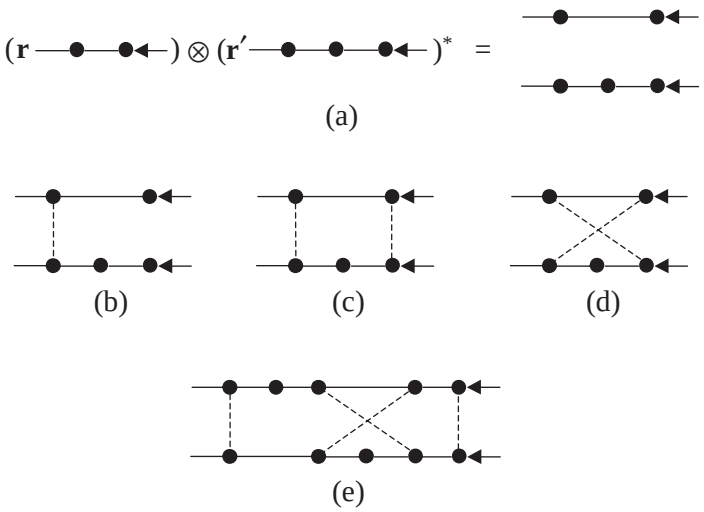

Fig. 8. Classification of terms entering the Twersky expansion of the dyadic correlation function.

indicates both the summation over all appropriate particles and the statistical averaging over the particle states and positions. According to Subsection 3.4, summing the upper paths yields the coherent field at $\mathbf{r}_1$. This result can be represented by the diagram shown in Fig. 9(b), in which the symbol $\Leftarrow$ denotes the coherent field.

Similarly, summing the upper paths of the diagram shown in panel (c) gives the diagram shown in panel (d). Indeed, since one particle is already reserved for the lower path, the number of particles contributing to the upper paths in panel (c) is $N-1$. However, the difference between the sum of the upper paths in panel (c) and the coherent field at $\mathbf{r}_1$ vanishes as N tends to infinity. We can continue this process and conclude that the total contribution of the diagrams with no connectors is given by the sum of the diagrams shown in panel (e). The final result can be represented by the diagram in panel (f), which means that the contribution of all the diagrams with no connectors to the dyadic correlation

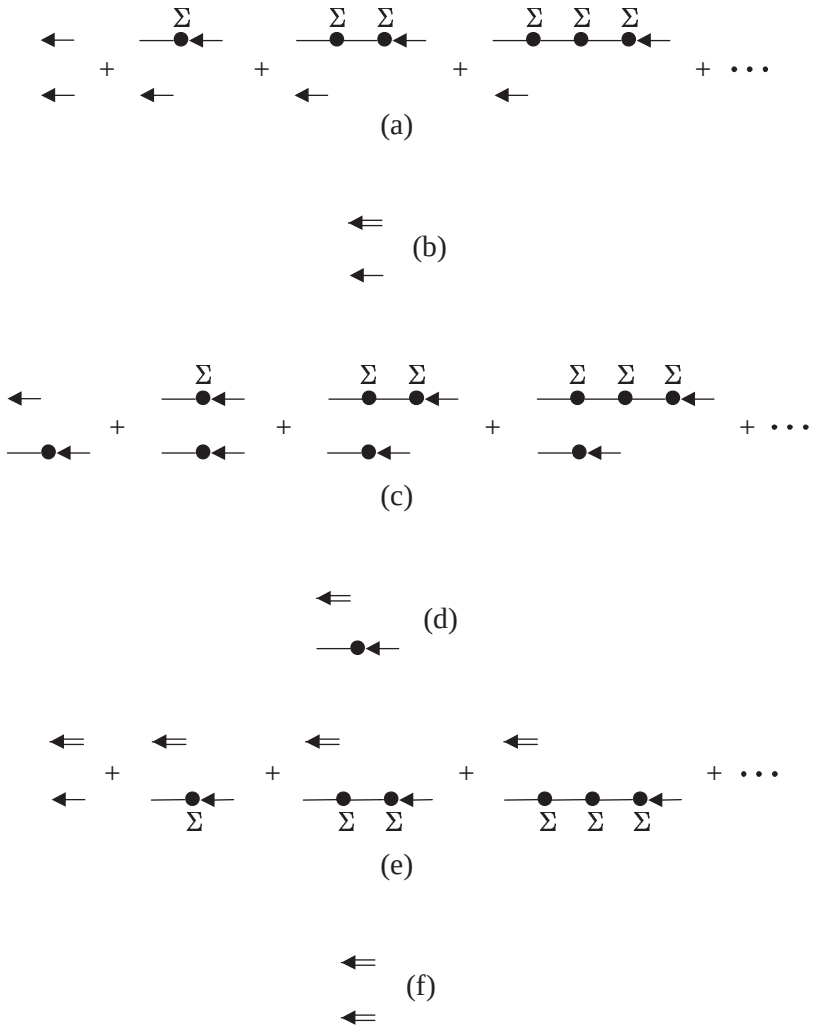

Fig. 9. Calculation of the total contribution of the diagrams with no connectors.

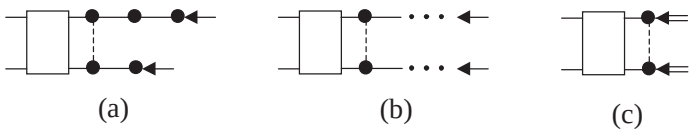

Fig. 10. Diagrams with one or more vertical connectors.

function is simply the dyadic product of the coherent fields at the points $\mathbf{r}$ and $\mathbf{r}'$: $\mathbf{E}_c(\mathbf{r}) \otimes \mathbf{E}_c^*(\mathbf{r}')$.

All other diagrams contributing to the dyadic correlation function have at least one

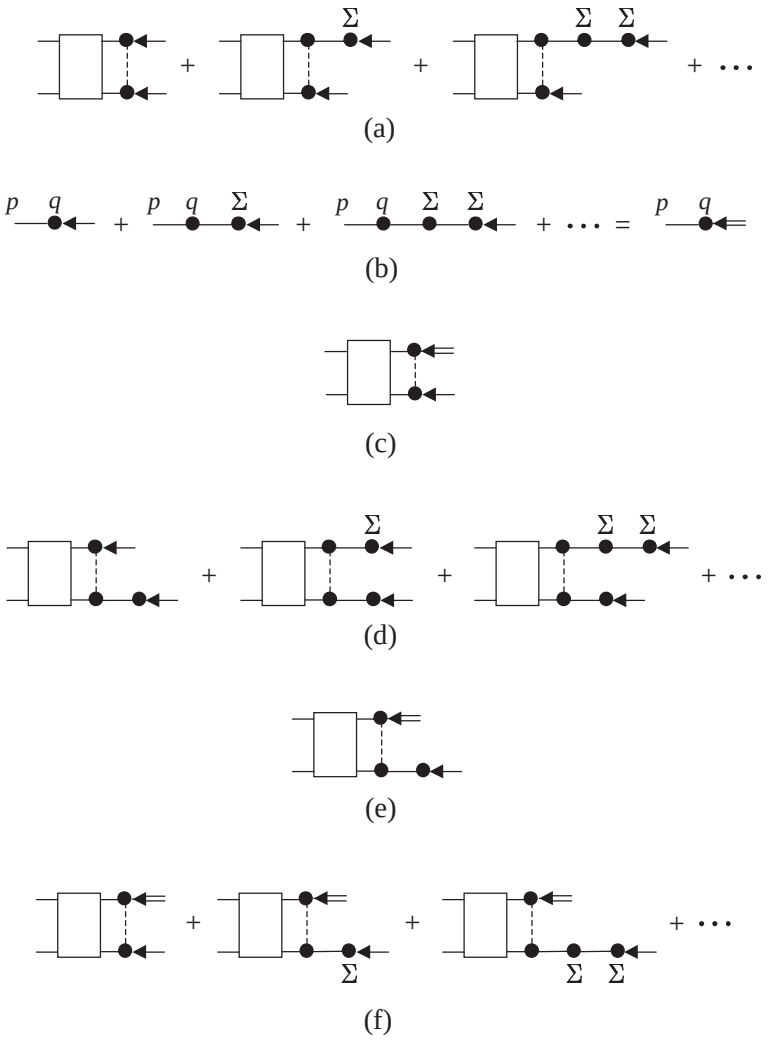

Fig. 11. Summation of the tails.

vertical connector, as shown in Fig. 10(a). The part of the diagram on the right-hand side of the right-most connector will be called the tail, whereas the box denotes the part of the diagram on the left-hand side of the right-most connector. The right-most common particle and the box form the body of the diagram.

Let us first consider the group of diagrams with the same body but with different tails, as shown in Fig. 10(b). We can repeat the derivation of subsection 3.4 and verify that the sum of all diagrams in Fig. 11(a) gives the diagram shown in Fig. 11(c). Indeed, let particle q be the right-most connected particle and particle p be the right-most particle on the left-hand side of particle q in the upper scattering paths of the diagrams shown in panel (a). The electric field created by particle q at the origin of particle p is represented by the sum of the diagrams on the left-hand side of panel (b). This result is summarized by the right-hand side of panel (b). Analogously, the sum of the diagrams in panel (d) is given by the diagram in panel (e), and so on. We can now sum up all diagrams in panel (f) and obtain the diagram shown in Fig. 10(c). Thus the total contribution to the dyadic correlation function of all the diagrams with the same body and all possible tails is equivalent to the contribution of a

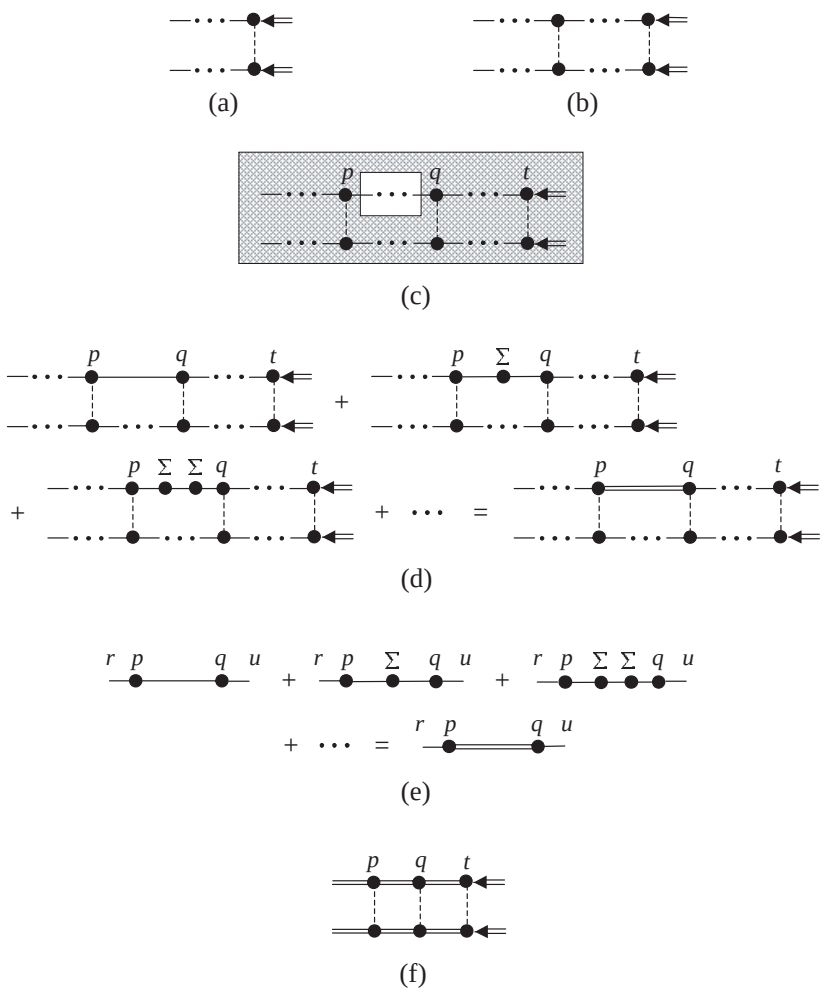

Fig. 12. Derivation of the ladder approximation for the dyadic correlation function.

single diagram formed by the body alone, *provided that the right-most common particle is excited by the coherent field rather than by the external incident field*. Thus we can cut off all tails and consider only truncated diagrams like those shown in Fig. 10(c).

Thus, the dyadic correlation function is equal to $\mathbf{E}_{\rm c}(\mathbf{r})\otimes\mathbf{E}_{\rm c}^{*}(\mathbf{r}')$ plus the statistical average of the sum of all connected diagrams of the type illustrated by panels (a)–(c) of Fig. 12, where the $\cdots$ denotes all possible combinations of unconnected particles. Let us, for example, consider the statistical average of the sum of all diagrams of the kind shown in panel (c) with the same fixed shaded part. We thus must evaluate the left-hand side of the equation shown in panel (d). Let particle *r* be the right-most particle on the left-hand side of particle *p* in the upper scattering paths of the diagrams on the left-hand side of panel (d) and *u* be the left-most particle on the right-hand side of particle *q*. The electric field created by particle *p* at the origin of particle *r* via all the diagrams shown on the left-hand side of panel (d) is given by the left-hand side of the equation shown diagrammatically in panel (e) and can be written in expanded form as

$$\begin{aligned}\mathbf{E}_r &= G(R_{rp})G(R_{pq})\vec{\vec{A}}_p(\hat{\mathbf{R}}_{rp},\hat{\mathbf{R}}_{pq})\cdot\vec{\vec{A}}_q(\hat{\mathbf{R}}_{pq},\hat{\mathbf{R}}_{qu})\cdot\mathbf{E}_q\\ &+\sum_i G(R_{rp})\Big\langle G(R_{pi})G(R_{iq})\vec{\vec{A}}_p(\hat{\mathbf{R}}_{rp},\hat{\mathbf{R}}_{pi})\cdot\vec{\vec{A}}_i(\hat{\mathbf{R}}_{pi},\hat{\mathbf{R}}_{iq})\cdot\vec{\vec{A}}_q(\hat{\mathbf{R}}_{iq},\hat{\mathbf{R}}_{qu})\Big\rangle\cdot\mathbf{E}_q\\ &+\sum_{ij} G(R_{rp})\Big\langle G(R_{pi})G(R_{ij})G(R_{jq})\vec{\vec{A}}_p(\hat{\mathbf{R}}_{rp},\hat{\mathbf{R}}_{pi})\cdot\vec{\vec{A}}_i(\hat{\mathbf{R}}_{pi},\hat{\mathbf{R}}_{ij})\cdot\vec{\vec{A}}_j(\hat{\mathbf{R}}_{ij},\hat{\mathbf{R}}_{jq})\\ &\cdot\vec{\vec{A}}_q(\hat{\mathbf{R}}_{jq},\hat{\mathbf{R}}_{qu})\Big\rangle\cdot\mathbf{E}_q+\cdots,\end{aligned}\tag{90}$$

where $\mathbf{E}_q$ is the field at the origin of particle *q* created by particle *u* and the summations and integrations are performed over all appropriate unconnected particles. In the limit $N\to\infty$, Eq. (90) takes the form

$$\begin{aligned}\mathbf{E}_r &= G(R_{rp})G(R_{pq})\vec{\vec{A}}_p(\hat{\mathbf{R}}_{rp},\hat{\mathbf{R}}_{pq})\cdot\vec{\vec{A}}_q(\hat{\mathbf{R}}_{pq},\hat{\mathbf{R}}_{qu})\cdot\mathbf{E}_q\\ &+n_0G(R_{rp})\int_V \mathrm{d}^3\mathbf{R}_i G(R_{pi})G(R_{iq})\vec{\vec{A}}_p(\hat{\mathbf{R}}_{rp},\hat{\mathbf{R}}_{pi})\cdot\Big\langle\vec{\vec{A}}(\hat{\mathbf{R}}_{pi},\hat{\mathbf{R}}_{iq})\Big\rangle\cdot\vec{\vec{A}}_q(\hat{\mathbf{R}}_{iq},\hat{\mathbf{R}}_{qu})\cdot\mathbf{E}_q\\ &+n_0^2G(R_{rp})\int_V \mathrm{d}^3\mathbf{R}_i\mathrm{d}^3\mathbf{R}_j G(R_{pi})G(R_{ij})G(R_{jq})\vec{\vec{A}}_p(\hat{\mathbf{R}}_{rp},\hat{\mathbf{R}}_{pi})\cdot\Big\langle\vec{\vec{A}}(\hat{\mathbf{R}}_{pi},\hat{\mathbf{R}}_{ij})\Big\rangle\\ &\cdot\Big\langle\vec{\vec{A}}(\hat{\mathbf{R}}_{ij},\hat{\mathbf{R}}_{jq})\Big\rangle\cdot\vec{\vec{A}}_q(\hat{\mathbf{R}}_{jq},\hat{\mathbf{R}}_{qu})\cdot\mathbf{E}_q\cdot\Big\langle\vec{\vec{A}}(\hat{\mathbf{R}}_{pq},\hat{\mathbf{R}}_{pq})\Big\rangle\cdot\vec{\vec{A}}_q(\hat{\mathbf{R}}_{pq},\hat{\mathbf{R}}_{qu})\cdot\mathbf{E}_{qu}.\end{aligned}\tag{91}$$

The integrals on the right-hand side of Eq. (91) can be evaluated using the method of stationary phase. The final result is [25]

$$\mathbf{E}_r = G(R_{rp})\vec{\vec{A}}_p(\hat{\mathbf{R}}_{rp},\hat{\mathbf{R}}_{pq})\cdot\frac{\vec{\vec{\eta}}(\hat{\mathbf{R}}_{pq},R_{pq})}{R_{pq}}\cdot\vec{\vec{A}}_q(\hat{\mathbf{R}}_{pq},\hat{\mathbf{R}}_{qu})\cdot\mathbf{E}_q,\tag{92}$$

where the coherent transmission dyad $\vec{\vec{\eta}}$ is given by Eq. (78). Obviously, this equation describes the coherent propagation of the wave scattered by particle *q* towards particle *p* through the scattering medium. The presence of other particles on the line of sight causes attenuation and, potentially, a change in polarization state of the wave.

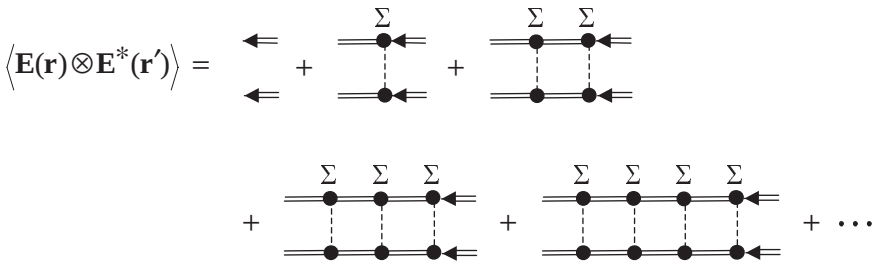

Fig. 13. Ladder approximation for the dyadic correlation function.

Equation (92) can be summarized by the diagram on the right-hand side of Fig. 12(e), where the double line indicates that the scalar factor $\exp[\mathrm{i}k_1 R_{pq}]/R_{pq}$ has been replaced by the dyadic factor $\exp[\mathrm{i}\vec{\kappa}(\hat{\mathbf{R}}_{pq})R_{pq}]/R_{pq}$. Thus the total contribution of all diagrams with three fixed common particles t, q, and p to the dyadic correlation function can be represented by the diagram in Fig. 12(f).

It is now clear that the final expression for the dyadic correlation function can be represented graphically by Fig. 13. Owing to their appearance, the diagrams on the right-hand side are called ladder diagrams, and this entire formula is called the ladder approximation for the dyadic correlation function.

3.7. INTEGRAL EQUATION FOR THE SPECIFIC COHERENCY DYAD

The coherency dyad is defined as $\vec{\vec{C}}(\mathbf{r}) = \mathbf{E}(\mathbf{r}) \otimes \mathbf{E}^*(\mathbf{r})$. The expanded form of the ladder approximation for the coherency dyad follows from Figs. 13 and 14:

$$\begin{aligned}\vec{\vec{C}}(\mathbf{r}) = \vec{\vec{C}}_{\mathrm{c}}(\mathbf{r}) &+ n_0 \int \mathrm{d}^3\mathbf{R}_1 \mathrm{d}\xi_1 \frac{\vec{\vec{\eta}}(\hat{\mathbf{r}}_1, r_1)}{r_1} \cdot \vec{\vec{A}}_1(\hat{\mathbf{r}}_1, \hat{\mathbf{s}}) \cdot \vec{\vec{C}}_{\mathrm{c}}(\mathbf{R}_1) \cdot \vec{\vec{A}}_1^{\mathrm{T}*}(\hat{\mathbf{r}}_1, \hat{\mathbf{s}}) \cdot \frac{\vec{\vec{\eta}}^{\mathrm{T}*}(\hat{\mathbf{r}}_1, r_1)}{r_1} \\ &+ n_0^2 \int \mathrm{d}^3\mathbf{R}_1 \mathrm{d}\xi_1 \int \mathrm{d}^3\mathbf{R}_2 \mathrm{d}\xi_2 \frac{\vec{\vec{\eta}}(\hat{\mathbf{r}}_1, r_1)}{r_1} \cdot \vec{\vec{A}}_1(\hat{\mathbf{r}}_1, \hat{\mathbf{R}}_{12}) \cdot \frac{\vec{\vec{\eta}}(\hat{\mathbf{R}}_{12}, R_{12})}{R_{12}} \cdot \vec{\vec{A}}_2(\hat{\mathbf{R}}_{12}, \hat{\mathbf{s}}) \\ &\cdot \vec{\vec{C}}_{\mathrm{c}}(\mathbf{R}_2) \cdot \vec{\vec{A}}_2^{\mathrm{T}*}(\hat{\mathbf{R}}_{12}, \hat{\mathbf{s}}) \cdot \frac{\vec{\vec{\eta}}^{\mathrm{T}*}(\hat{\mathbf{R}}_{12}, R_{12})}{R_{12}} \cdot \vec{\vec{A}}_1^{\mathrm{T}*}(\hat{\mathbf{r}}_1, \hat{\mathbf{R}}_{12}) \cdot \frac{\vec{\vec{\eta}}^{\mathrm{T}*}(\hat{\mathbf{r}}_1, r_1)}{r_1} + \cdots, \end{aligned} \tag{93}$$

where $\vec{\vec{C}}_{\mathrm{c}}(\mathbf{r}) = \mathbf{E}_{\mathrm{c}}(\mathbf{r}) \otimes \mathbf{E}_{\mathrm{c}}^*(\mathbf{r})$ is the coherent part of the coherency dyad. It is convenient to integrate over all positions of particle 1 using a local coordinate system with origin at the observation point, integrate over all positions of particle 2 using a local coordinate system with origin at the origin of particle 1, etc. Using the notation introduced in Fig. 14 yields

$$\vec{\vec{C}}(\mathbf{r}) = \int_{4\pi} \mathrm{d}\hat{\mathbf{p}} \vec{\vec{\Sigma}}(\mathbf{r}, -\hat{\mathbf{p}}), \tag{94}$$

where $\vec{\vec{\Sigma}}(\mathbf{r}, -\hat{\mathbf{p}})$ is the specific coherency dyad defined by

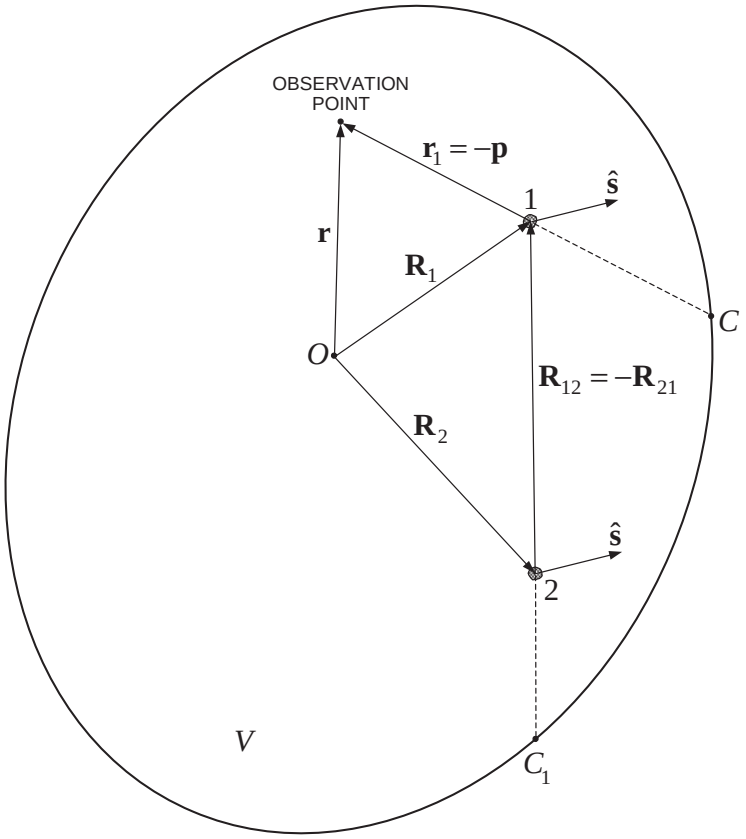

Fig. 14. Geometry showing the quantities used in Eq. (93).

$$
\begin{aligned}
\vec{\Sigma}(\mathbf{r},-\hat{\mathbf{p}}) &= \delta(\hat{\mathbf{p}}+\hat{\mathbf{s}})\vec{C}_{\mathrm{c}}(\mathbf{r}) \\
&\quad + n_0 \int \mathrm{d}p\, \mathrm{d}\xi_1\, \vec{\eta}(-\hat{\mathbf{p}},p)\cdot\vec{A}_1(-\hat{\mathbf{p}},\hat{\mathbf{s}})\cdot\vec{C}_{\mathrm{c}}(\mathbf{r}+\mathbf{p})\cdot\vec{A}_1^{\mathrm{T}*}(-\hat{\mathbf{p}},\hat{\mathbf{s}})\cdot\vec{\eta}^{\,\mathrm{T}*}(-\hat{\mathbf{p}},p) \\
&\quad + n_0^2 \int \mathrm{d}p\, \mathrm{d}\xi_1 \int \mathrm{d}R_{21}\mathrm{d}\hat{\mathbf{R}}_{21}\mathrm{d}\xi_2 \vec{\eta}(-\hat{\mathbf{p}},p)\cdot\vec{A}_1(-\hat{\mathbf{p}},-\hat{\mathbf{R}}_{21})\cdot\vec{\eta}(-\hat{\mathbf{R}}_{21},R_{21}) \\
&\qquad \cdot\vec{A}_2(-\hat{\mathbf{R}}_{21},\hat{\mathbf{s}})\cdot\vec{C}_{\mathrm{c}}(\mathbf{r}+\mathbf{p}+\mathbf{R}_{21})\cdot\vec{A}_2^{\mathrm{T}*}(-\hat{\mathbf{R}}_{21},\hat{\mathbf{s}})\cdot\vec{\eta}^{\,\mathrm{T}*}(-\hat{\mathbf{R}}_{21},R_{21}) \\
&\qquad \cdot\vec{A}_1^{\mathrm{T}*}(-\hat{\mathbf{p}},-\hat{\mathbf{R}}_{21})\cdot\vec{\eta}^{\,\mathrm{T}*}(-\hat{\mathbf{p}},p)+\cdots . \qquad (95)
\end{aligned}
$$

Note that p ranges from zero at the observation point to the corresponding value at the point where the straight line in the $\hat{\mathbf{p}}$-direction crosses the boundary of the medium (point C in Fig. 14), R_{21} ranges from zero at the origin of particle 1 to the corresponding value at point C_1, etc. The specific coherency dyad has the dimension of specific intensity ($\mathrm{Wm^{-2}sr^{-1}}$) rather than that of monochromatic energy flux.

It is straightforward to verify that $\vec{\Sigma}$ satisfies the following integral equation:

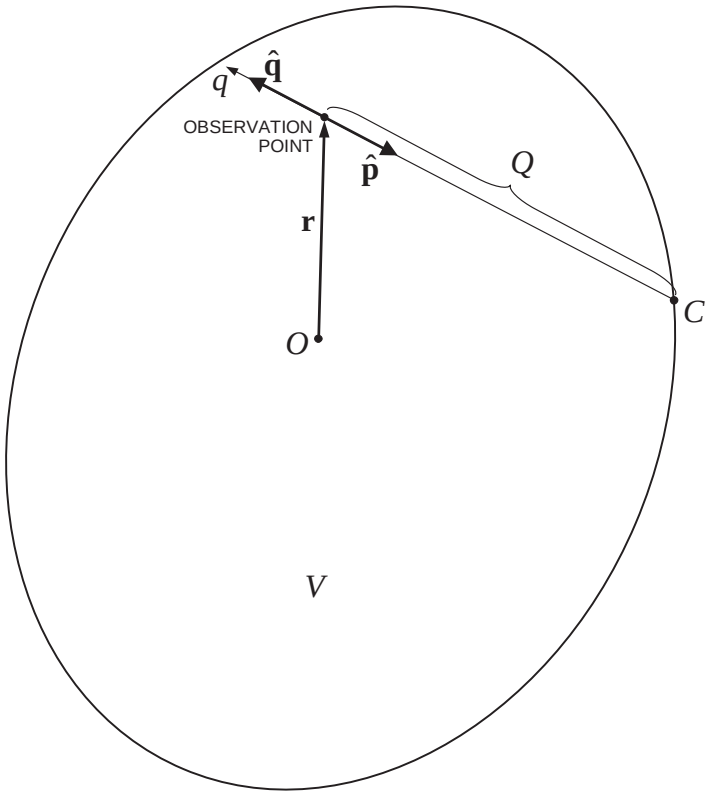

Fig. 15. Geometry showing the quantities used in the derivation of the RTE.

$$\vec{\Sigma}(\mathbf{r},-\hat{\mathbf{p}}) = \delta(\hat{\mathbf{p}}+\hat{\mathbf{s}})\vec{C}_{\mathrm{c}}(\mathbf{r}) + n_0 \int \mathrm{d}p\, \mathrm{d}\xi\, \mathrm{d}\hat{\mathbf{p}}'\, \vec{\eta}(-\hat{\mathbf{p}}, p)\cdot \vec{A}(-\hat{\mathbf{p}},-\hat{\mathbf{p}}')\cdot \vec{\Sigma}(\mathbf{r}+\mathbf{p},-\hat{\mathbf{p}}')$$
$$\cdot\, \vec{A}^{\mathrm{T}*}(-\hat{\mathbf{p}},-\hat{\mathbf{p}}')\cdot \vec{\eta}^{\mathrm{T}*}(-\hat{\mathbf{p}}, p)\,. \qquad (96)$$

Indeed, Eq. (95) is reproduced by iterating Eq. (96). Equation (95) is simply an order-of-scattering expansion of the specific coherency dyad *with coherent field serving as the source of multiple scattering*.

The interpretation of Eq. (96) is clear: the specific coherency dyad for a direction $-\hat{\mathbf{p}}$ at a point $\mathbf{r}$ consists of a coherent part and an incoherent part. The latter is a cumulative contribution of all particles located along the straight line in the $\hat{\mathbf{p}}$-direction and scattering radiation coming from all directions $-\hat{\mathbf{p}}'$ into the direction $-\hat{\mathbf{p}}$.

3.8 RTE FOR SPECIFIC COHERENCY DYAD

We now introduce a q-axis as shown in Fig. 15 and rewrite Eq. (96) as

$$\vec{\Sigma}(Q,\hat{\mathbf{q}}) = \delta(\hat{\mathbf{q}}-\hat{\mathbf{s}})\vec{C}_{\mathrm{c}}(Q) + n_0 \int_0^Q \mathrm{d}q \int \mathrm{d}\xi \int_{4\pi} \mathrm{d}\hat{\mathbf{q}}'\, \vec{\eta}(\hat{\mathbf{q}}, Q-q)\cdot \vec{A}(\hat{\mathbf{q}},\hat{\mathbf{q}}')$$

$$\cdot \ddot{\Sigma}(q,\hat{\mathbf{q}}') \cdot \ddot{A}^{\mathrm{T}*}(\hat{\mathbf{q}},\hat{\mathbf{q}}') \cdot \ddot{\eta}^{\mathrm{T}*}(\hat{\mathbf{q}},Q-q)\,. \tag{97}$$

Defining the diffuse specific coherency dyad as $\ddot{\Sigma}_{\mathrm{d}}(Q,\hat{\mathbf{q}}) = \ddot{\Sigma}(Q,\hat{\mathbf{q}}) - \delta(\hat{\mathbf{q}}-\hat{\mathbf{s}})\ddot{C}_{\mathrm{c}}(Q)$, we obtain

$$\begin{aligned}\ddot{\Sigma}_{\mathrm{d}}(Q,\hat{\mathbf{q}}) = n_0 \int_0^Q \mathrm{d}q \int \mathrm{d}\xi\, \ddot{\eta}(\hat{\mathbf{q}},Q-q) \cdot \ddot{A}(\hat{\mathbf{q}},\hat{\mathbf{s}}) \ddot{C}_{\mathrm{c}}(q) \cdot \ddot{A}^{\mathrm{T}*}(\hat{\mathbf{q}},\hat{\mathbf{s}}) \cdot \ddot{\eta}^{\mathrm{T}*}(\hat{\mathbf{q}},Q-q) \\ + n_0 \int_0^Q \mathrm{d}q \int \mathrm{d}\xi \int_{4\pi} \mathrm{d}\hat{\mathbf{q}}'\, \ddot{\eta}(\hat{\mathbf{q}},Q-q) \cdot \ddot{A}(\hat{\mathbf{q}},\hat{\mathbf{q}}') \cdot \ddot{\Sigma}_{\mathrm{d}}(q,\hat{\mathbf{q}}') \\ \cdot \ddot{A}^{\mathrm{T}*}(\hat{\mathbf{q}},\hat{\mathbf{q}}') \cdot \ddot{\eta}^{\mathrm{T}*}(\hat{\mathbf{q}},Q-q)\,.\end{aligned} \tag{98}$$

Differentiating both sides of Eq. (98) yields

$$\begin{aligned}\frac{\mathrm{d}\ddot{\Sigma}_{\mathrm{d}}(Q,\hat{\mathbf{q}})}{\mathrm{d}Q} = \mathrm{i}\ddot{\kappa}(\hat{\mathbf{q}}) \cdot \ddot{\Sigma}_{\mathrm{d}}(Q,\hat{\mathbf{q}}) - \mathrm{i}\ddot{\Sigma}_{\mathrm{d}}(Q,\hat{\mathbf{q}}) \cdot \ddot{\kappa}^{\mathrm{T}*}(\hat{\mathbf{q}}) \\ + n_0 \int \mathrm{d}\xi \int_{4\pi} \mathrm{d}\hat{\mathbf{q}}' \ddot{A}(\hat{\mathbf{q}},\hat{\mathbf{q}}') \cdot \ddot{\Sigma}_{\mathrm{d}}(Q,\hat{\mathbf{q}}') \cdot \ddot{A}^{\mathrm{T}*}(\hat{\mathbf{q}},\hat{\mathbf{q}}') \\ + n_0 \int \mathrm{d}\xi \ddot{A}(\hat{\mathbf{q}},\hat{\mathbf{s}}) \cdot \ddot{C}_{\mathrm{c}}(Q) \cdot \ddot{A}^{\mathrm{T}*}(\hat{\mathbf{q}},\hat{\mathbf{s}})\,.\end{aligned} \tag{99}$$

For further use, it is more convenient to rewrite Eq. (99) in the following form:

$$\begin{aligned}\frac{\mathrm{d}\ddot{\Sigma}_{\mathrm{d}}(\mathbf{r},\hat{\mathbf{q}})}{\mathrm{d}q} = \mathrm{i}\ddot{\kappa}(\hat{\mathbf{q}}) \cdot \ddot{\Sigma}_{\mathrm{d}}(\mathbf{r},\hat{\mathbf{q}}) - \mathrm{i}\ddot{\Sigma}_{\mathrm{d}}(\mathbf{r},\hat{\mathbf{q}}) \cdot \ddot{\kappa}^{\mathrm{T}*}(\hat{\mathbf{q}}) \\ + n_0 \int \mathrm{d}\xi \int_{4\pi} \mathrm{d}\hat{\mathbf{q}}' \ddot{A}(\hat{\mathbf{q}},\hat{\mathbf{q}}') \cdot \ddot{\Sigma}_{\mathrm{d}}(\mathbf{r},\hat{\mathbf{q}}') \cdot \ddot{A}^{\mathrm{T}*}(\hat{\mathbf{q}},\hat{\mathbf{q}}') \\ + n_0 \int \mathrm{d}\xi \ddot{A}(\hat{\mathbf{q}},\hat{\mathbf{s}}) \cdot \ddot{C}_{\mathrm{c}}(\mathbf{r}) \cdot \ddot{A}^{\mathrm{T}*}(\hat{\mathbf{q}},\hat{\mathbf{s}})\,,\end{aligned} \tag{100}$$

where dq is measured along the unit vector $\hat{\mathbf{q}}$. Equation (100) is the integro-differential RTE for the diffuse specific coherency dyad.

3.9. RTE FOR SPECIFIC INTENSITY VECTOR

It follows from Eq. (98) that $\hat{\mathbf{q}} \cdot \ddot{\Sigma}_{\mathrm{d}}(\mathbf{r},\hat{\mathbf{q}}) = \ddot{\Sigma}_{\mathrm{d}}(\mathbf{r},\hat{\mathbf{q}}) \cdot \hat{\mathbf{q}} = 0$, which allows us to introduce the 2×2 diffuse specific coherency matrix $\tilde{\boldsymbol{\rho}}_{\mathrm{d}}$ using the local coordinate system with origin at the observation point and orientation identical to that of the laboratory coordinate system:

$$\tilde{\boldsymbol{\rho}}_{\mathrm{d}}(\mathbf{r},\hat{\mathbf{q}}) = \frac{1}{2}\sqrt{\frac{\varepsilon_1}{\mu_0}} \begin{bmatrix} \hat{\boldsymbol{\theta}}(\hat{\mathbf{q}}) \cdot \ddot{\Sigma}_{\mathrm{d}}(\mathbf{r},\hat{\mathbf{q}}) \cdot \hat{\boldsymbol{\theta}}(\hat{\mathbf{q}}) & \hat{\boldsymbol{\theta}}(\hat{\mathbf{q}}) \cdot \ddot{\Sigma}_{\mathrm{d}}(\mathbf{r},\hat{\mathbf{q}}) \cdot \hat{\boldsymbol{\varphi}}(\hat{\mathbf{q}}) \\ \hat{\boldsymbol{\varphi}}(\hat{\mathbf{q}}) \cdot \ddot{\Sigma}_{\mathrm{d}}(\mathbf{r},\hat{\mathbf{q}}) \cdot \hat{\boldsymbol{\theta}}(\hat{\mathbf{q}}) & \hat{\boldsymbol{\varphi}}(\hat{\mathbf{q}}) \cdot \ddot{\Sigma}_{\mathrm{d}}(\mathbf{r},\hat{\mathbf{q}}) \cdot \hat{\boldsymbol{\varphi}}(\hat{\mathbf{q}}) \end{bmatrix}. \tag{101}$$

We can now rewrite Eq. (100) in the form of the RTE for the diffuse specific coherency matrix:

$$\frac{\mathrm{d}\widetilde{\boldsymbol{\rho}}_{\mathrm{d}}(\mathbf{r},\hat{\mathbf{q}})}{\mathrm{d}q} = \mathrm{i}\mathbf{k}(\hat{\mathbf{q}})\widetilde{\boldsymbol{\rho}}_{\mathrm{d}}(\mathbf{r},\hat{\mathbf{q}}) - \mathrm{i}\widetilde{\boldsymbol{\rho}}_{\mathrm{d}}(\mathbf{r},\hat{\mathbf{q}})\mathbf{k}^{\mathrm{T}*}(\hat{\mathbf{q}})$$
$$+ n_0 \int \mathrm{d}\xi \int_{4\pi} \mathrm{d}\hat{\mathbf{q}}'\mathbf{S}(\hat{\mathbf{q}},\hat{\mathbf{q}}')\widetilde{\boldsymbol{\rho}}_{\mathrm{d}}(\mathbf{r},\hat{\mathbf{q}}')\mathbf{S}^{\mathrm{T}*}(\hat{\mathbf{q}},\hat{\mathbf{q}}')$$
$$+ n_0 \int \mathrm{d}\xi \mathbf{S}(\hat{\mathbf{q}},\hat{\mathbf{s}})\boldsymbol{\rho}_{\mathrm{c}}(\mathbf{r})\mathbf{S}^{\mathrm{T}*}(\hat{\mathbf{q}},\hat{\mathbf{s}}) , \tag{102}$$

where $\mathbf{S}$ is the amplitude matrix, $\mathbf{k}$ is the matrix propagation constant given by Eq. (82), and

$$\boldsymbol{\rho}_{\mathrm{c}}(\mathbf{r}) = \frac{1}{2}\sqrt{\frac{\varepsilon_1}{\mu_0}}\begin{bmatrix} \hat{\boldsymbol{\theta}}(\hat{\mathbf{s}})\cdot\vec{\vec{C}}_{\mathrm{c}}(\mathbf{r})\cdot\hat{\boldsymbol{\theta}}(\hat{\mathbf{s}}) & \hat{\boldsymbol{\theta}}(\hat{\mathbf{s}})\cdot\vec{\vec{C}}_{\mathrm{c}}(\mathbf{r})\cdot\hat{\boldsymbol{\varphi}}(\hat{\mathbf{s}}) \\ \hat{\boldsymbol{\varphi}}(\hat{\mathbf{s}})\cdot\vec{\vec{C}}_{\mathrm{c}}(\mathbf{r})\cdot\hat{\boldsymbol{\theta}}(\hat{\mathbf{s}}) & \hat{\boldsymbol{\varphi}}(\hat{\mathbf{s}})\cdot\vec{\vec{C}}_{\mathrm{c}}(\mathbf{r})\cdot\hat{\boldsymbol{\varphi}}(\hat{\mathbf{s}}) \end{bmatrix}. \tag{103}$$

The next obvious step is to introduce the corresponding coherency column vectors $\widetilde{\mathbf{J}}_{\mathrm{d}}$ and $\mathbf{J}_{\mathrm{c}}$:

$$\widetilde{\mathbf{J}}_{\mathrm{d}}(\mathbf{r},\hat{\mathbf{q}}) = \begin{bmatrix} \widetilde{\rho}_{\mathrm{d}11}(\mathbf{r},\hat{\mathbf{q}}) \\ \widetilde{\rho}_{\mathrm{d}12}(\mathbf{r},\hat{\mathbf{q}}) \\ \widetilde{\rho}_{\mathrm{d}21}(\mathbf{r},\hat{\mathbf{q}}) \\ \widetilde{\rho}_{\mathrm{d}22}(\mathbf{r},\hat{\mathbf{q}}) \end{bmatrix}, \qquad \mathbf{J}_{\mathrm{c}}(\mathbf{r}) = \begin{bmatrix} \rho_{\mathrm{c}11}(\mathbf{r}) \\ \rho_{\mathrm{c}12}(\mathbf{r}) \\ \rho_{\mathrm{c}21}(\mathbf{r}) \\ \rho_{\mathrm{c}22}(\mathbf{r}) \end{bmatrix}. \tag{104}$$

Lengthy, but simple algebraic manipulations yield

$$\frac{\mathrm{d}\widetilde{\mathbf{J}}_{\mathrm{d}}(\mathbf{r},\hat{\mathbf{q}})}{\mathrm{d}q} = -n_0\left\langle \mathbf{K}^J(\hat{\mathbf{q}})\right\rangle\widetilde{\mathbf{J}}_{\mathrm{d}}(\mathbf{r},\hat{\mathbf{q}}) + n_0\int_{4\pi}\mathrm{d}\hat{\mathbf{q}}'\left\langle \mathbf{Z}^J(\hat{\mathbf{q}},\hat{\mathbf{q}}')\right\rangle\widetilde{\mathbf{J}}_{\mathrm{d}}(\mathbf{r},\hat{\mathbf{q}}')$$
$$+ n_0\left\langle \mathbf{Z}^J(\hat{\mathbf{q}},\hat{\mathbf{s}})\right\rangle\mathbf{J}_{\mathrm{c}}(\mathbf{r}) , \tag{105}$$

where $\left\langle \mathbf{K}^J(\hat{\mathbf{q}})\right\rangle$ is the coherency extinction matrix averaged over the particle states and $\left\langle \mathbf{Z}^J(\hat{\mathbf{q}},\hat{\mathbf{q}}')\right\rangle$ is the ensemble average of the coherency phase matrix. The column vector $\mathbf{J}_{\mathrm{c}}(\mathbf{r})$ satisfies the transfer equation (85).

The final step in the derivation of the RTE is to define the diffuse specific intensity column vector, $\widetilde{\mathbf{I}}_{\mathrm{d}}(\mathbf{r},\hat{\mathbf{q}}) = \mathbf{D}\widetilde{\mathbf{J}}_{\mathrm{d}}(\mathbf{r},\hat{\mathbf{q}})$, and the coherent Stokes column vector, $\mathbf{I}_{\mathrm{c}}(\mathbf{r}) = \mathbf{D}\mathbf{J}_{\mathrm{c}}(\mathbf{r})$, and rewrite Eq. (105) in the form

$$\frac{\mathrm{d}\widetilde{\mathbf{I}}_{\mathrm{d}}(\mathbf{r},\hat{\mathbf{q}})}{\mathrm{d}q} = -n_0\left\langle \mathbf{K}(\hat{\mathbf{q}})\right\rangle\widetilde{\mathbf{I}}_{\mathrm{d}}(\mathbf{r},\hat{\mathbf{q}}) + n_0\int_{4\pi}\mathrm{d}\hat{\mathbf{q}}'\left\langle \mathbf{Z}(\hat{\mathbf{q}},\hat{\mathbf{q}}')\right\rangle\widetilde{\mathbf{I}}_{\mathrm{d}}(\mathbf{r},\hat{\mathbf{q}}') + n_0\left\langle \mathbf{Z}(\hat{\mathbf{q}},\hat{\mathbf{s}})\right\rangle\mathbf{I}_{\mathrm{c}}(\mathbf{r}) , \tag{106}$$

where $\left\langle \mathbf{K}(\hat{\mathbf{q}})\right\rangle$ is the ensemble average of the Stokes extinction matrix and $\left\langle \mathbf{Z}(\hat{\mathbf{q}},\hat{\mathbf{q}}')\right\rangle$ is the ensemble average of the Stokes phase matrix. The coherent Stokes column vector $\mathbf{I}_{\mathrm{c}}(\mathbf{r})$ satisfies the transfer equation (86).

3.10. DISCUSSION

Equations (86) and (106) represent the classical form of the RTE applicable to arbitrarily shaped and arbitrarily oriented particles. The microphysical derivation of these equations outlined above is based on fundamental principles of statistical electromagnetics and naturally replaces the original incident field as the source of multiple scattering by the decaying coherent field and leads to the introduction of the diffuse specific intensity vector describing the photometric and polarimetric characteristics of the multiply scattered light. The physical interpretation of $\widetilde{\mathbf{I}}_{\rm d}(\mathbf{r},\hat{\mathbf{q}})$ is rather transparent. Imagine a collimated detector centered at the observation point and aligned along the direction $\hat{\mathbf{q}}$ $(\neq\hat{\mathbf{s}})$ (Fig. 16). Let ΔS be the detector area and $\Delta\Omega$ its acceptance solid angle. Each infinitesimal element of the detector surface responds to the radiant energy coming from the directions confined to a narrow cone with the small solid-angle aperture $\Delta\Omega$ centered around $\hat{\mathbf{q}}$. On the other hand, we can use Eq. (98) to write

$$\Delta\Omega\,\widetilde{\mathbf{I}}_{\rm d}(\mathbf{r},\hat{\mathbf{q}}) \approx n_0 \int_{\Delta V} {\rm d}^3\mathbf{p}\,\frac{1}{p^2}\mathbf{H}(\hat{\mathbf{q}},p) \times\left(\left\langle \boldsymbol{Z}(\hat{\mathbf{q}},\hat{\mathbf{s}})\right\rangle \mathbf{I}_{\rm c}(\mathbf{r}+\mathbf{p}) + \int_{4\pi} {\rm d}\hat{\mathbf{q}}'\left\langle \mathbf{Z}(\hat{\mathbf{q}},\hat{\mathbf{q}}')\right\rangle \widetilde{\mathbf{I}}_{\rm d}(\mathbf{r}+\mathbf{p},\hat{\mathbf{q}}')\right), \qquad (107)$$

where $\mathbf{p}$ originates at the observation point $\mathbf{r}$ (Fig. 15) and the integration is performed

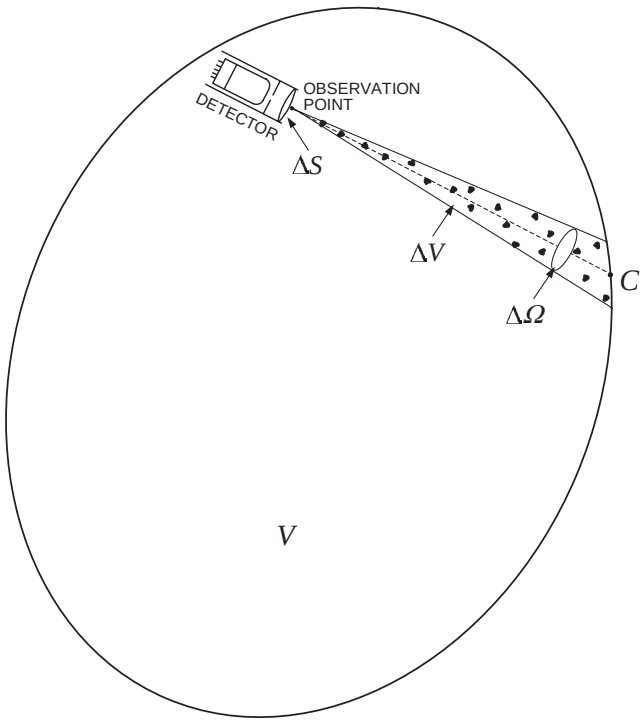

Fig. 16. Physical meaning of the diffuse specific intensity vector.

over the conical volume element ΔV having the solid-angle aperture $\Delta\Omega$ and extending from the observation point to point C (Fig. 16). The right-hand side of Eq. (107) is simply the integral of the scattering signal per unit surface area perpendicular to $\hat{\mathbf{q}}$ per unit time over all particles contained in the conical volume element. It is now clear what quantity describes the total polarized signal measured by the detector per unit time: it is the product $\Delta S\Delta\Omega\,\widetilde{\mathbf{I}}_{\mathrm{d}}(\mathbf{r},\hat{\mathbf{q}})$, which has the dimension of power (W). The first element of $\widetilde{\mathbf{I}}_{\mathrm{d}}(\mathbf{r},\hat{\mathbf{q}})$ is the standard diffuse specific intensity $\widetilde{I}_{\mathrm{d}}(\mathbf{r},\hat{\mathbf{q}})$ defined such that the product $\Delta t\Delta S\Delta\Omega\,\widetilde{I}_{\mathrm{d}}(\mathbf{r},\hat{\mathbf{q}})$ gives the amount of radiant energy transported in a time interval Δt through an element of surface area ΔS normal to $\hat{\mathbf{q}}$ in directions confined to a solid angle element $\Delta\Omega$ centered around $\hat{\mathbf{q}}$. The fact that the diffuse specific intensity vector can be measured by an optical device and computed theoretically by solving the RTE explains the practical usefulness of this quantity.

The microphysical derivation of the RTE was based on the following fundamental approximations:

- We assumed that each particle is located in the far-field zones of all other particles and that the observation point is also located in the far-field zones of all the particles forming the scattering medium.
- We neglected all scattering paths going through a particle two and more times (the Twersky approximation).
- We assumed that the position and state of each particle are statistically independent of each other and of those of all other particles and that the spatial distribution of the particles throughout the medium is random and statistically uniform.
- We assumed that the scattering medium is convex, which assured that a wave exiting the medium cannot re-enter it.
- We assumed that the number of particles N forming the scattering medium is large.
- We ignored all diagrams with crossing connectors in the diagrammatic expansion of the dyadic correlation function (the ladder approximation).

As a consequence, the RTE does not describe interference effects such as coherent backscattering. The latter is caused by constructive interference of pairs of conjugate waves propagating along the same scattering paths but in opposite directions and is represented by diagrams with crossing connectors excluded from the derivation [21, 23]. Particles that are randomly positioned and are separated widely enough that each of them is located in the far-field zones of all other particles are traditionally called independent scatterers [26]. Thus the requirement of independent scattering is a necessary condition of validity of the radiative transfer theory.

A fundamental property of the RTE is that it satisfies the energy conservation law. Indeed, we can rewrite Eqs. (86) and (106) as a single RTE:

$$\hat{\mathbf{q}}\cdot\nabla\widetilde{\mathbf{I}}(\mathbf{r},\hat{\mathbf{q}})=\nabla\cdot[\hat{\mathbf{q}}\widetilde{\mathbf{I}}(\mathbf{r},\hat{\mathbf{q}})]=-n_0\left\langle\mathbf{K}(\hat{\mathbf{q}})\right\rangle\widetilde{\mathbf{I}}(\mathbf{r},\hat{\mathbf{q}})+n_0\int_{4\pi}\mathrm{d}\hat{\mathbf{q}}'\left\langle\mathbf{Z}(\hat{\mathbf{q}},\hat{\mathbf{q}}')\right\rangle\widetilde{\mathbf{I}}(\mathbf{r},\hat{\mathbf{q}}'),\quad(108)$$

where $\widetilde{\mathbf{I}}(\mathbf{r},\hat{\mathbf{q}}) = \delta(\hat{\mathbf{q}}-\hat{\mathbf{s}})\mathbf{I}_{\rm c}(\mathbf{r}) + \widetilde{\mathbf{I}}_{\rm d}(\mathbf{r},\hat{\mathbf{q}})$ is the full specific intensity vector. The flux density vector is defined as $\mathbf{F}(\mathbf{r}) = \int_{4\pi} {\rm d}\hat{\mathbf{q}}\,\hat{\mathbf{q}}\widetilde{I}(\mathbf{r},\hat{\mathbf{q}})$. The product $\hat{\mathbf{p}}\cdot\mathbf{F}(\mathbf{r}){\rm d}S$ gives the amount and the direction of the net flow of power through a surface element dS normal to $\hat{\mathbf{p}}$. Integrating both sides of Eq. (108) over all directions $\hat{\mathbf{q}}$ and recalling the definitions of the extinction, scattering, and absorption cross sections (Subsection 2.5), we derive

$$-\nabla\cdot\mathbf{F}(\mathbf{r}) = n_0 \int_{4\pi} {\rm d}\hat{\mathbf{q}} \langle C_{\rm abs}(\hat{\mathbf{q}})\rangle \widetilde{I}(\mathbf{r},\mathbf{q}) . \qquad (109)$$

This means that the net inflow of electromagnetic power per unit volume is equal to the total power absorbed per unit volume. If the particles forming the scattering medium are nonabsorbing so that $\langle C_{\rm abs}(\hat{\mathbf{q}})\rangle = 0$, then the flux density vector is divergence-free: $\nabla\cdot\mathbf{F}(\mathbf{r}) = 0$.

For macroscopically isotropic and mirror-symmetric media, Eq. (108) can be significantly simplified (see Subsection 2.7):

$$\frac{{\rm d}\widetilde{\mathbf{I}}(\mathbf{r};\theta,\varphi)}{{\rm d}\tau} = -\widetilde{\mathbf{I}}(\mathbf{r};\theta,\varphi) + \frac{\varpi}{4\pi}\int_{-1}^{+1}{\rm d}(\cos\theta')\int_0^{2\pi}{\rm d}\varphi'\,\widetilde{\mathbf{Z}}(\theta,\theta',\varphi-\varphi')\,\widetilde{\mathbf{I}}(\mathbf{r};\theta',\varphi') , \quad (110)$$

where ${\rm d}\tau = n_0\langle C_{\rm ext}\rangle {\rm d}q$ is the optical pathlength element. By writing the normalized phase matrix in the form $\widetilde{\mathbf{Z}}(\theta,\theta',\varphi-\varphi')$, we explicitly indicate that it depends on the difference of the azimuth angles of the scattering and incident directions rather than on their specific values. Equation (110) can be made even simpler by neglecting polarization and replacing the specific intensity vector by its first element (i.e., specific intensity), and the normalized phase matrix by its (1, 1) element (i.e., the phase function):

$$\frac{{\rm d}\widetilde{I}(\mathbf{r};\theta,\varphi)}{{\rm d}\tau(\mathbf{r})} = -\widetilde{I}(\mathbf{r};\theta,\varphi) + \frac{\varpi}{4\pi}\int_{-1}^{+1}{\rm d}(\cos\theta')\int_0^{2\pi}{\rm d}\varphi'\,a_1(\Theta)\,\widetilde{I}(\mathbf{r};\theta',\varphi') , \qquad (111)$$

where Θ is the scattering angle (Fig. 3). Although ignoring the vector nature of light and replacing the exact vector radiative transfer equation by its approximate scalar counterpart has no rigorous physical justification, this simplification is widely used when the medium is illuminated by unpolarized light and only the intensity of multiply scattered light is required. The scalar approximation gives poor accuracy when the size of the scattering particles is much smaller than the wavelength [29], but provides acceptable results for particles comparable to and larger than the wavelength [30].

4. Adding equations

In order to apply the RTT to analyses of laboratory measurements or remote sensing observations, one needs efficient theoretical techniques for solving the RTE. Unfortunately, like many integro-differential equations, the RTE is difficult to study mathematically and numerically. In order to facilitate the analysis, we will need several simplifying assumptions. The most important of them are that the scattering medium (i)

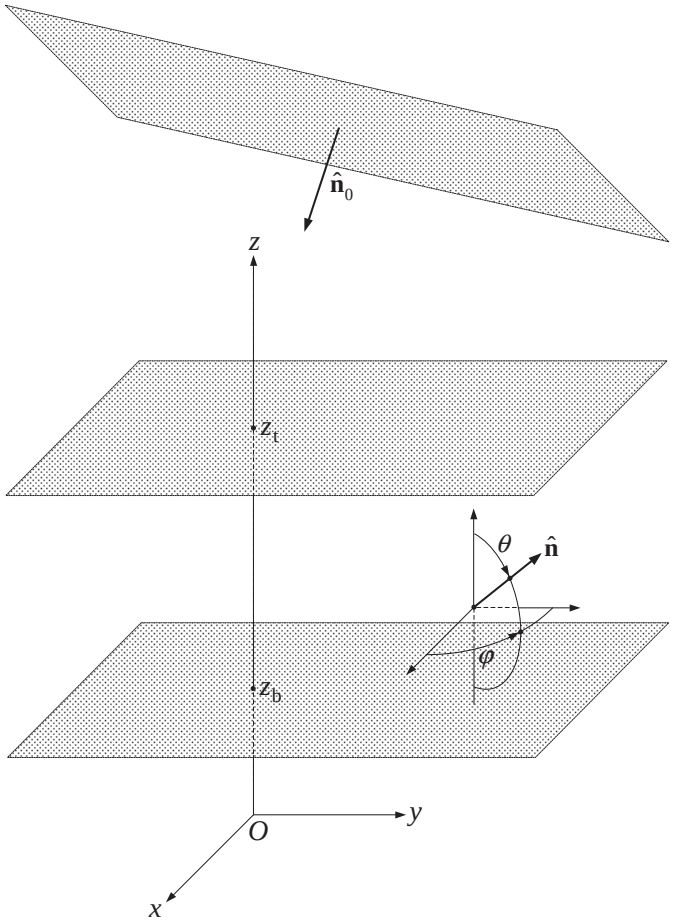

Fig. 17. Plane-parallel scattering medium illuminated by a parallel quasi-monochromatic beam of light.

is plane parallel, (ii) has an infinite horizontal extent, and (iii) is illuminated from above by a parallel quasi-monochromatic beam of light. These assumptions mean that all properties of the medium and of the radiation field may vary only in the vertical direction and are independent of the horizontal coordinates. Taken together, these assumptions specify the so-called *standard problem* of atmospheric optics and provide a model relevant to a great variety of applications in diverse fields of science and technology. In this section we will not make any further assumptions and will derive several important equations describing the internal diffuse radiation field as well as the diffuse radiation exiting the medium.

4.1. THE STANDARD PROBLEM

Let us consider a plane-parallel layer extending in the vertical direction from $z = z_b$ to $z = z_t$, where the z-axis of the laboratory coordinate system is perpendicular to the boundaries of the medium and is directed upwards, and "b" and "t" stand for "bottom" and "top," respectively (Fig. 17). A propagation direction $\hat{\mathbf{n}}$ at a point in space will be

specified by a couplet $\{u,\varphi\}$, where $u=-\cos\theta\in[-1,+1]$ is the direction cosine, and θ and φ are the corresponding polar and azimuth angles with respect to the local coordinate system having the same spatial orientation as the laboratory coordinate system. It is also convenient to introduce a non-negative quantity $\mu=|u|\in[0,1]$. In order to make many formulas of this section more compact, we will denote by $\hat{\mu}$ the pair of arguments (μ,φ) and by $-\hat{\mu}$ the pair of arguments $(-\mu,\varphi)$ (note that $\hat{\mu}$ and $-\hat{\mu}$ are not unit vectors). A $\hat{\mu}$ always corresponds to a downward direction and a $-\hat{\mu}$ always corresponds to an upward direction. We also denote

$$\int \mathrm{d}\hat{\mu}=\int_0^1 \mathrm{d}\mu\int_0^{2\pi}\mathrm{d}\varphi\,. \tag{112}$$

Let us assume that the scattering layer is illuminated from above by a parallel quasi-monochromatic beam of light propagating in the direction $\hat{\mathbf{n}}_0=\{\mu_0,\varphi_0\}$. The uniformity and the infinite transverse extent of the beam ensure that all parameters of the internal radiation field and those of the radiation leaving the scattering layer are independent of the coordinates *x* and *y*. Therefore, Eq. (108) can be rewritten in the form

$$-u\frac{\mathrm{d}\widetilde{\mathbf{I}}(z,\hat{\mathbf{n}})}{\mathrm{d}z}=-n_0(z)\mathbf{K}(z,\hat{\mathbf{n}})\widetilde{\mathbf{I}}(z,\hat{\mathbf{n}})+n_0(z)\int_{4\pi}\mathrm{d}\hat{\mathbf{n}}'\,\mathbf{Z}(z,\hat{\mathbf{n}},\hat{\mathbf{n}}')\widetilde{\mathbf{I}}(z,\hat{\mathbf{n}}') \tag{113}$$

and must be supplemented by the boundary conditions

$$\widetilde{\mathbf{I}}(z_{\mathrm{t}},\hat{\mu})=\delta(\mu-\mu_0)\delta(\varphi-\varphi_0)\mathbf{I}_0\,, \tag{114}$$

$$\widetilde{\mathbf{I}}(z_{\mathrm{b}},-\hat{\mu})=\mathbf{0}\,, \tag{115}$$

where $\widetilde{\mathbf{I}}(z,\hat{\mathbf{n}})=\delta(\hat{\mathbf{n}}-\hat{\mathbf{n}}_0)\mathbf{I}_{\mathrm{c}}(z)+\widetilde{\mathbf{I}}_{\mathrm{d}}(z,\hat{\mathbf{n}})$ is the full specific intensity vector including both the coherent and the diffuse component, $\mathbf{K}$ and $\mathbf{Z}$ are the ensemble-averaged extinction and phase matrices, respectively (note that we have omitted the angular brackets for the sake of brevity), $\mathbf{I}_0$ is the Stokes vector of the incident beam, and $\mathbf{0}$ is a zero four-element column. The boundary conditions follow directly from the integral form of the RTE and mean that the downwelling radiation at the upper boundary of the layer consists only of the incident parallel beam and that there is no upwelling radiation at the lower boundary. Equations (113)–(115) collectively represent what we have called the *standard problem*.

Since $n_0(z)$ is a common factor in both terms on the right-hand side of Eq. (113), it is convenient to eliminate it by introducing a new vertical "coordinate" $\psi(z)$ according to $\mathrm{d}\psi=-n_0(z)\mathrm{d}z$ or

$$\psi(z)=\int_z^\infty n_0(z')\mathrm{d}z'\,. \tag{116}$$

The $\psi(z)$ has the dimension m^{-2} and is the number of particles in a vertical column having a unit cross section and extending from $z'=z$ to infinity. It is, therefore, natural to call it the "particle depth." Unlike the *z*-coordinate, which increases in the upward direction, the ψ-coordinate increases in the downward direction. We then have

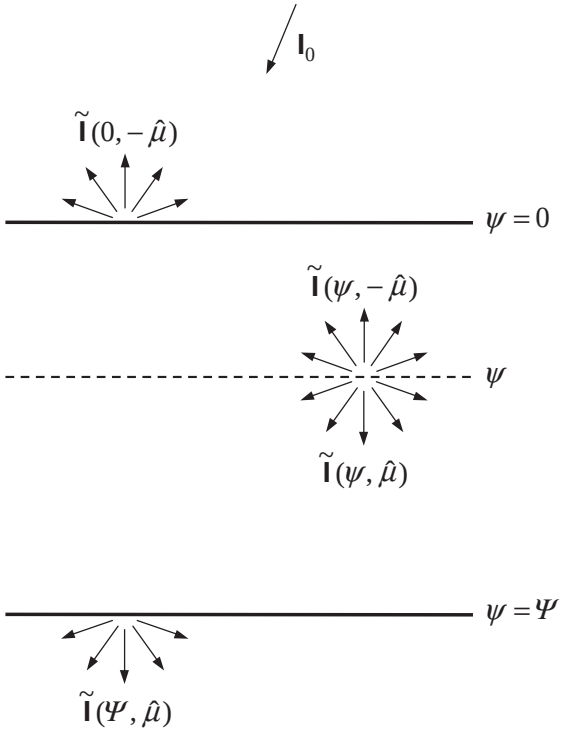

Fig. 18. The standard problem.

$$u\frac{\mathrm{d}\tilde{\mathbf{I}}(\psi,\hat{\mathbf{n}})}{\mathrm{d}\psi} = -\mathbf{K}(\psi,\hat{\mathbf{n}})\tilde{\mathbf{I}}(\psi,\hat{\mathbf{n}}) + \int_{4\pi}\mathrm{d}\hat{\mathbf{n}}'\,\mathbf{Z}(\psi,\hat{\mathbf{n}},\hat{\mathbf{n}}')\tilde{\mathbf{I}}(\psi,\hat{\mathbf{n}}'), \tag{117}$$

$$\tilde{\mathbf{I}}(0,\hat{\mu}) = \delta(\mu-\mu_0)\delta(\varphi-\varphi_0)\mathbf{I}_0, \tag{118}$$

$$\tilde{\mathbf{I}}(\Psi,-\hat{\mu}) = \mathbf{0}, \tag{119}$$

where $\Psi = \psi(z_\mathrm{b})$ is the "particle thickness" of the layer (Fig. 18).

4.2. THE MATRIZANT

Consider first the solution of the differential transfer equation

$$\mu\frac{\mathrm{d}\tilde{\mathbf{I}}(\psi,\hat{\mu})}{\mathrm{d}\psi} = -\mathbf{K}(\psi,\hat{\mu})\tilde{\mathbf{I}}(\psi,\hat{\mu}), \qquad \psi \geq \psi_0 \tag{120}$$

supplemented by the initial condition

$$\tilde{\mathbf{I}}(\psi_0,\hat{\mu}) = \tilde{\mathbf{I}}_0. \tag{121}$$

It is convenient to express $\tilde{\mathbf{I}}(\psi,\hat{\mu})$ in terms of the solution of the following auxiliary initial-value problem:

$$\mu \frac{\mathrm{d}\mathbf{X}(\psi, \psi_0, \hat{\mu})}{\mathrm{d}\psi} = -\mathbf{K}(\psi, \hat{\mu})\mathbf{X}(\psi, \psi_0, \hat{\mu}), \qquad \psi \geq \psi_0 , \tag{122}$$

$$\mathbf{X}(\psi_0, \psi_0, \hat{\mu}) = \boldsymbol{\Delta} , \tag{123}$$

where $\mathbf{X}(\psi, \psi_0, \hat{\mu})$ is a 4×4 real matrix called the matrizant and $\boldsymbol{\Delta} = \mathrm{diag}[1,1,1,1]$ is the 4×4 unit matrix. Specifically, if the matrizant is known then the solution of Eqs. (120)–(121) is simply

$$\widetilde{\mathbf{I}}(\psi, \hat{\mu}) = \mathbf{X}(\psi, \psi_0, \hat{\mu})\widetilde{\mathbf{I}}_0 . \tag{124}$$

The matrizant has the obvious property

$$\mathbf{X}(\psi, \psi_0, \hat{\mu}) = \mathbf{X}(\psi, \psi_1, \hat{\mu})\mathbf{X}(\psi_1, \psi_0, \hat{\mu}) , \tag{125}$$

where $\psi_0 \leq \psi_1 \leq \psi$.

If the scattering layer is homogeneous then $\mathbf{K}(\psi, \hat{\mu}) \equiv \mathbf{K}(\hat{\mu})$, and the matrizant can be written in the form of a matrix exponent:

$$\mathbf{X}(\psi, \psi_0, \hat{\mu}) = \exp\left[-(\psi - \psi_0)\,\mathbf{K}(\hat{\mu})/\mu\right] . \tag{126}$$

If the layer is inhomogeneous, one should exploit the property (125) by subdividing the interval $[\psi_0, \psi]$ into a number N of equal subintervals $[\psi_0, \psi_1]$, …, $[\psi_{n-1}, \psi_n]$, …, $[\psi_{N-1}, \psi]$ and calculating the matrizant in the limit $N \to \infty$:

$$\begin{aligned}\mathbf{X}(\psi, \psi_0, \hat{\mu}) = \lim_{N\to\infty} \Big\{ &\left[\boldsymbol{\Delta} - (\Delta\psi/\mu)\,\mathbf{K}(\psi_{N-1} + \Delta\psi/2, \hat{\mu})\right]\cdots \\ &\times\left[\boldsymbol{\Delta} - (\Delta\psi/\mu)\,\mathbf{K}(\psi_{n-1} + \Delta\psi/2, \hat{\mu})\right]\cdots \\ &\times\left[\boldsymbol{\Delta} - (\Delta\psi/\mu)\,\mathbf{K}(\psi_0 + \Delta\psi/2, \hat{\mu})\right]\Big\} ,\end{aligned} \tag{127}$$

where $\Delta\psi = (\psi - \psi_0)/N$.

Similarly, the solution of the equation

$$-\mu \frac{\mathrm{d}\widetilde{\mathbf{I}}(\psi, -\hat{\mu})}{\mathrm{d}\psi} = -\mathbf{K}(\psi, -\hat{\mu})\widetilde{\mathbf{I}}(\psi, -\hat{\mu}), \qquad \psi \leq \psi_0 \tag{128}$$

supplemented by the initial condition

$$\widetilde{\mathbf{I}}(\psi_0, -\hat{\mu}) = \widetilde{\mathbf{I}}_0 \tag{129}$$

can be expressed in terms of the solution of the auxiliary initial-value problem

$$-\mu \frac{\mathrm{d}\mathbf{X}(\psi, \psi_0, -\hat{\mu})}{\mathrm{d}\psi} = -\mathbf{K}(\psi, -\hat{\mu})\mathbf{X}(\psi, \psi_0, -\hat{\mu}), \qquad \psi \leq \psi_0 , \tag{130}$$

$$\mathbf{X}(\psi_0, \psi_0, -\hat{\mu}) = \boldsymbol{\Delta} \tag{131}$$

as

$$\widetilde{\mathbf{I}}(\psi,-\hat{\mu})=\mathbf{X}(\psi,\psi_0,-\hat{\mu})\widetilde{\mathbf{I}}_0\,. \tag{132}$$

The matrizant $\mathbf{X}(\psi,\psi_0,-\hat{\mu})$ has the property

$$\mathbf{X}(\psi,\psi_0,-\hat{\mu})=\mathbf{X}(\psi,\psi_1,-\hat{\mu})\mathbf{X}(\psi_1,\psi_0,-\hat{\mu}),\qquad \psi\le\psi_1\le\psi_0 \tag{133}$$

and is given by

$$\mathbf{X}(\psi,\psi_0,-\hat{\mu})=\exp\left[-(\psi_0-\psi)\,\mathbf{K}(-\hat{\mu})/\mu\right] \tag{134}$$

if the layer is homogeneous and by

$$\begin{aligned}\mathbf{X}(\psi,\psi_0,-\hat{\mu})=\lim_{N\to\infty}\Big\{&\left[\boldsymbol{\Delta}-(\Delta\psi/\mu)\,\mathbf{K}(\psi_{N-1}-\Delta\psi/2,-\hat{\mu})\right]\cdots\\ &\times\left[\boldsymbol{\Delta}-(\Delta\psi/\mu)\,\mathbf{K}(\psi_{n-1}-\Delta\psi/2,-\hat{\mu})\right]\cdots\\ &\times\left[\boldsymbol{\Delta}-(\Delta\psi/\mu)\,\mathbf{K}(\psi_0-\Delta\psi/2,-\hat{\mu})\right]\Big\}\end{aligned} \tag{135}$$

if the layer is inhomogeneous, where $\Delta\psi=(\psi_0-\psi)/N$ and $\psi_n=\psi_0-n\Delta\psi$.

4.3. THE GENERAL PROBLEM

The standard problem (117)–(119) implies that the scattering layer is illuminated only from above and only by a parallel beam of light. It is useful, however, to consider mathematically the following more general boundary values, which include the boundary conditions (118) and (119) as a particular case:

$$\widetilde{\mathbf{I}}(0,\hat{\mu})=\widetilde{\mathbf{I}}_{\downarrow}(\hat{\mu})\,, \tag{136}$$

$$\widetilde{\mathbf{I}}(\Psi,-\hat{\mu})=\widetilde{\mathbf{I}}_{\uparrow}(-\hat{\mu})\,, \tag{137}$$

where $\widetilde{\mathbf{I}}_{\downarrow}(\hat{\mu})$ and $\widetilde{\mathbf{I}}_{\uparrow}(-\hat{\mu})$ are arbitrary. We will call Eqs. (117), (136), and (137) the *general problem*.

The linearity of the RTE allows us to express the radiation field $\widetilde{\mathbf{I}}(\psi,\hat{\mathbf{n}})$ for $\psi\in[0,\Psi]$ in terms of the specific intensity vectors $\widetilde{\mathbf{I}}_{\downarrow}(\hat{\mu})$ and $\widetilde{\mathbf{I}}_{\uparrow}(-\hat{\mu})$ as follows:

$$\begin{aligned}\widetilde{\mathbf{I}}(\psi,\hat{\mu})=\mathbf{X}(\psi,0,\hat{\mu})\widetilde{\mathbf{I}}_{\downarrow}(\hat{\mu})&+\tfrac{1}{\pi}\int\mathrm{d}\hat{\mu}'\mu'\mathbf{D}(\psi,\hat{\mu},\hat{\mu}')\widetilde{\mathbf{I}}_{\downarrow}(\hat{\mu}')\\ &+\tfrac{1}{\pi}\int\mathrm{d}\hat{\mu}'\mu'\mathbf{U}^{\dagger}(\psi,\hat{\mu},\hat{\mu}')\widetilde{\mathbf{I}}_{\uparrow}(-\hat{\mu}')\,,\end{aligned} \tag{138}$$

$$\begin{aligned}\widetilde{\mathbf{I}}(\psi,-\hat{\mu})=\mathbf{X}(\psi,\Psi,-\hat{\mu})\widetilde{\mathbf{I}}_{\uparrow}(-\hat{\mu})&+\tfrac{1}{\pi}\int\mathrm{d}\hat{\mu}'\mu'\mathbf{U}(\psi,\hat{\mu},\hat{\mu}')\widetilde{\mathbf{I}}_{\downarrow}(\hat{\mu}')\\ &+\tfrac{1}{\pi}\int\mathrm{d}\hat{\mu}'\mu'\mathbf{D}^{\dagger}(\psi,\hat{\mu},\hat{\mu}')\widetilde{\mathbf{I}}_{\uparrow}(-\hat{\mu}')\,,\end{aligned} \tag{139}$$

where the 4×4 matrices $\mathbf{D}$ and $\mathbf{U}$ describe the response of the scattering layer to the radiation incident on the upper boundary from above, while the 4×4 matrices $\mathbf{D}^{\dagger}$ and $\mathbf{U}^{\dagger}$

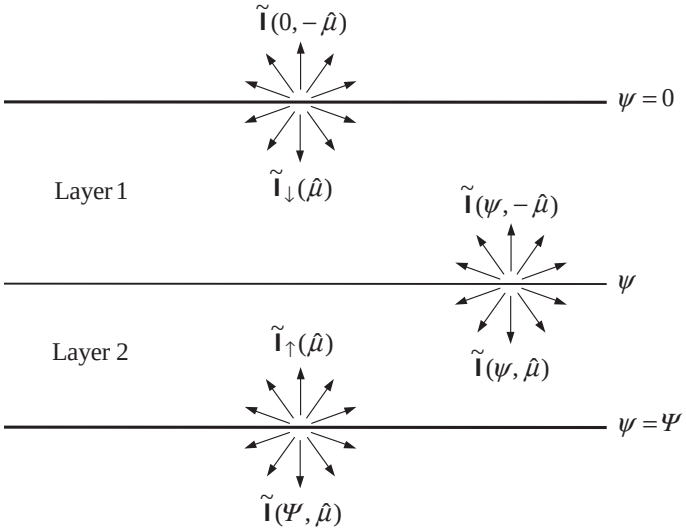

Fig. 19. Illustration of the adding principle.

describe the response to the radiation illuminating the bottom boundary of the layer from below. The first terms on the right-hand side of Eqs. (138) and (139) describe the coherent propagation of the incident light, whereas the remaining terms describe the result of multiple scattering. The corresponding reflection and transmission matrices determine the Stokes parameters of the radiation exiting the layer and are defined as

$$\mathbf{R}(\hat{\mu},\hat{\mu}') = \mathbf{U}(0,\hat{\mu},\hat{\mu}') , \tag{140}$$

$$\mathbf{T}(\hat{\mu},\hat{\mu}') = \mathbf{D}(\Psi,\hat{\mu},\hat{\mu}') , \tag{141}$$

$$\mathbf{R}^{\dagger}(\hat{\mu},\hat{\mu}') = \mathbf{U}^{\dagger}(\Psi,\hat{\mu},\hat{\mu}') , \tag{142}$$

$$\mathbf{T}^{\dagger}(\hat{\mu},\hat{\mu}') = \mathbf{D}^{\dagger}(0,\hat{\mu},\hat{\mu}') . \tag{143}$$

The matrices $\mathbf{R}$ and $\mathbf{T}$ describe the response of the layer to the external radiation falling from above, whereas the matrices $\mathbf{R}^{\dagger}$ and $\mathbf{T}^{\dagger}$ describe the response to the external radiation falling from below.

The reader can easily verify that the solution of the standard problem can now be expressed as

$$\tilde{\mathbf{I}}(\psi,\hat{\mu}) = \delta(\mu-\mu_0)\delta(\varphi-\varphi_0)\mathbf{X}(\psi,0,\hat{\mu}_0)\mathbf{I}_0 + \tfrac{1}{\pi}\mu_0\mathbf{D}(\psi,\hat{\mu},\hat{\mu}_0)\mathbf{I}_0 , \tag{144}$$

$$\tilde{\mathbf{I}}(\psi,-\hat{\mu}) = \tfrac{1}{\pi}\mu_0\mathbf{U}(\psi,\hat{\mu},\hat{\mu}_0)\mathbf{I}_0 , \tag{145}$$

$$\tilde{\mathbf{I}}(\Psi,\hat{\mu}) = \delta(\mu-\mu_0)\delta(\varphi-\varphi_0)\mathbf{X}(\Psi,0,\hat{\mu}_0)\mathbf{I}_0 + \tfrac{1}{\pi}\mu_0\mathbf{T}(\hat{\mu},\hat{\mu}_0)\mathbf{I}_0 , \tag{146}$$

$$\tilde{\mathbf{I}}(0,-\hat{\mu}) = \tfrac{1}{\pi}\mu_0\mathbf{R}(\hat{\mu},\hat{\mu}_0)\mathbf{I}_0 . \tag{147}$$

4.4. ADDING EQUATIONS

In this subsection we will describe an elegant mathematical scheme for computing the matrices $\mathbf{D}$, $\mathbf{U}$, $\mathbf{D}^{\dagger}$, $\mathbf{U}^{\dagger}$, $\mathbf{R}$, $\mathbf{T}$, $\mathbf{R}^{\dagger}$, and $\mathbf{T}^{\dagger}$ based on so-called adding equations. Let us

divide the entire layer $[0,\Psi]$ into layers $[0,\psi]$ and $[\psi,\Psi]$ (Fig. 19). Applying Eqs. (138)–(143) to the two component layers and to the combined layer yields

$$\mathbf{U}(\psi,\hat{\mu},\hat{\mu}') = \mathbf{R}_2(\hat{\mu},\hat{\mu}')\mathbf{X}(\psi,0,\hat{\mu}') + \tfrac{1}{\pi}\int \mathrm{d}\hat{\mu}''\mu''\,\mathbf{R}_2(\hat{\mu},\hat{\mu}'')\mathbf{D}(\psi,\hat{\mu}'',\hat{\mu}')\,, \tag{148}$$

$$\mathbf{D}(\psi,\hat{\mu},\hat{\mu}') = \mathbf{T}_1(\hat{\mu},\hat{\mu}') + \tfrac{1}{\pi}\int \mathrm{d}\hat{\mu}''\mu''\,\mathbf{R}_1^{\dagger}(\hat{\mu},\hat{\mu}'')\mathbf{U}(\psi,\hat{\mu}'',\hat{\mu}')\,, \tag{149}$$

$$\mathbf{U}^{\dagger}(\psi,\hat{\mu},\hat{\mu}') = \mathbf{R}_1^{\dagger}(\hat{\mu},\hat{\mu}')\mathbf{X}(\psi,\Psi,-\hat{\mu}') + \tfrac{1}{\pi}\int \mathrm{d}\hat{\mu}''\mu''\,\mathbf{R}_1^{\dagger}(\hat{\mu},\hat{\mu}'')\mathbf{D}^{\dagger}(\psi,\hat{\mu}'',\hat{\mu}')\,, \tag{150}$$

$$\mathbf{D}^{\dagger}(\psi,\hat{\mu},\hat{\mu}') = \mathbf{T}_2^{\dagger}(\hat{\mu},\hat{\mu}') + \tfrac{1}{\pi}\int \mathrm{d}\hat{\mu}''\mu''\,\mathbf{R}_2(\hat{\mu},\hat{\mu}'')\mathbf{U}^{\dagger}(\psi,\hat{\mu}'',\hat{\mu}')\,, \tag{151}$$

where the subscripts 1 and 2 denote the reflection and transmission matrices of isolated layers 1 and 2, respectively. Indeed, we can apply Eqs. (138), (141), and (142) to layer 1 and write

$$\begin{aligned}
\widetilde{\mathbf{I}}(\psi,\hat{\mu}) &= \mathbf{X}(\psi,0,\hat{\mu})\widetilde{\mathbf{I}}_{\downarrow}(\hat{\mu}) + \tfrac{1}{\pi}\int \mathrm{d}\hat{\mu}'\mu'\,\mathbf{T}_1(\hat{\mu},\hat{\mu}')\widetilde{\mathbf{I}}_{\downarrow}(\hat{\mu}') \\
&\quad + \tfrac{1}{\pi}\int \mathrm{d}\hat{\mu}'\mu'\,\mathbf{R}_1^{\dagger}(\hat{\mu},\hat{\mu}')\widetilde{\mathbf{I}}(\psi,-\hat{\mu}') \\
&= \mathbf{X}(\psi,0,\hat{\mu})\widetilde{\mathbf{I}}_{\downarrow}(\hat{\mu}) + \tfrac{1}{\pi}\int \mathrm{d}\hat{\mu}'\mu'\,\mathbf{T}_1(\hat{\mu},\hat{\mu}')\widetilde{\mathbf{I}}_{\downarrow}(\hat{\mu}') \\
&\quad + \tfrac{1}{\pi}\int \mathrm{d}\hat{\mu}'\mu'\,\mathbf{R}_1^{\dagger}(\hat{\mu},\hat{\mu}')\Big[\mathbf{X}(\psi,\Psi,-\hat{\mu}')\widetilde{\mathbf{I}}_{\uparrow}(-\hat{\mu}') + \tfrac{1}{\pi}\int \mathrm{d}\hat{\mu}''\mu''\,\mathbf{U}(\psi,\hat{\mu}',\hat{\mu}'')\widetilde{\mathbf{I}}_{\downarrow}(\hat{\mu}'') \\
&\qquad + \tfrac{1}{\pi}\int \mathrm{d}\hat{\mu}''\mu''\,\mathbf{D}^{\dagger}(\psi,\hat{\mu}',\hat{\mu}'')\widetilde{\mathbf{I}}_{\uparrow}(-\hat{\mu}'')\Big]\,,
\end{aligned} \tag{152}$$

which, after comparison with Eq. (138), gives Eqs. (149) and (150). Similarly, Eqs. (148) and (151) follow from

$$\begin{aligned}
\widetilde{\mathbf{I}}(\psi,-\hat{\mu}) &= \mathbf{X}(\psi,\Psi,-\hat{\mu})\widetilde{\mathbf{I}}_{\uparrow}(-\hat{\mu}) + \tfrac{1}{\pi}\int \mathrm{d}\hat{\mu}'\mu'\,\mathbf{T}_2^{\dagger}(\hat{\mu},\hat{\mu}')\widetilde{\mathbf{I}}_{\uparrow}(-\hat{\mu}') \\
&\quad + \tfrac{1}{\pi}\int \mathrm{d}\hat{\mu}'\mu'\,\mathbf{R}_2(\hat{\mu},\hat{\mu}')\widetilde{\mathbf{I}}(\psi,\hat{\mu}') \\
&= \mathbf{X}(\psi,\Psi,-\hat{\mu})\widetilde{\mathbf{I}}_{\uparrow}(-\hat{\mu}) + \tfrac{1}{\pi}\int \mathrm{d}\hat{\mu}'\mu'\,\mathbf{T}_2^{\dagger}(\hat{\mu},\hat{\mu}')\widetilde{\mathbf{I}}_{\uparrow}(-\hat{\mu}') \\
&\quad + \tfrac{1}{\pi}\int \mathrm{d}\hat{\mu}'\mu'\,\mathbf{R}_2(\hat{\mu},\hat{\mu}')\Big[\mathbf{X}(\psi,0,\hat{\mu}')\widetilde{\mathbf{I}}_{\downarrow}(\hat{\mu}') + \tfrac{1}{\pi}\int \mathrm{d}\hat{\mu}''\mu''\,\mathbf{D}(\psi,\hat{\mu}',\hat{\mu}'')\widetilde{\mathbf{I}}_{\downarrow}(\hat{\mu}'') \\
&\qquad + \tfrac{1}{\pi}\int \mathrm{d}\hat{\mu}''\mu''\,\mathbf{U}^{\dagger}(\psi,\hat{\mu}',\hat{\mu}'')\widetilde{\mathbf{I}}_{\uparrow}(-\hat{\mu}'')\Big]
\end{aligned} \tag{153}$$

and Eq. (139). By analogy, one can derive

$$\begin{aligned}
\mathbf{R}(\hat{\mu},\hat{\mu}') &= \mathbf{R}_1(\hat{\mu},\hat{\mu}') + \mathbf{X}(0,\psi,-\hat{\mu})\mathbf{U}(\psi,\hat{\mu},\hat{\mu}') \\
&\quad + \tfrac{1}{\pi}\int \mathrm{d}\hat{\mu}''\mu''\,\mathbf{T}_1^{\dagger}(\hat{\mu},\hat{\mu}'')\mathbf{U}(\psi,\hat{\mu}'',\hat{\mu}')\,,
\end{aligned} \tag{154}$$

$$\begin{aligned}
\mathbf{T}(\hat{\mu},\hat{\mu}') &= \mathbf{T}_2(\hat{\mu},\hat{\mu}')\mathbf{X}(\psi,0,\hat{\mu}') + \mathbf{X}(\Psi,\psi,\hat{\mu})\mathbf{D}(\psi,\hat{\mu},\hat{\mu}') \\
&\quad + \tfrac{1}{\pi}\int \mathrm{d}\hat{\mu}''\mu''\,\mathbf{T}_2(\hat{\mu},\hat{\mu}'')\mathbf{D}(\psi,\hat{\mu}'',\hat{\mu}')\,,
\end{aligned} \tag{155}$$

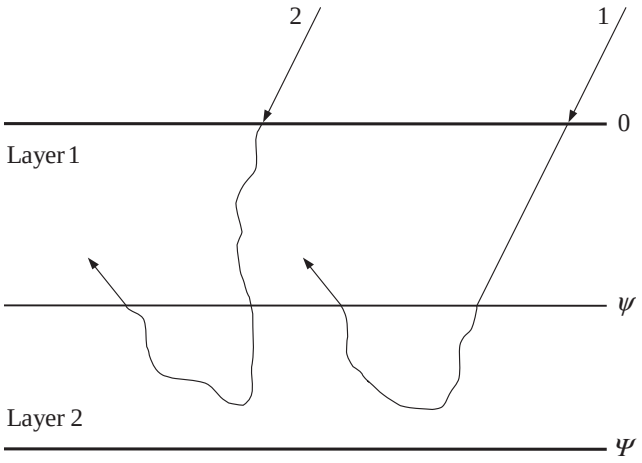

Fig. 20. Physical interpretation of Eq. (148).

$$\mathbf{R}^{\dagger}(\hat{\mu},\hat{\mu}') = \mathbf{R}_2^{\dagger}(\hat{\mu},\hat{\mu}') + \mathbf{X}(\Psi,\psi,\hat{\mu})\mathbf{U}^{\dagger}(\psi,\hat{\mu},\hat{\mu}') + \tfrac{1}{\pi}\int \mathrm{d}\hat{\mu}''\mu''\,\mathbf{T}_2(\hat{\mu},\hat{\mu}'')\mathbf{U}^{\dagger}(\psi,\hat{\mu}'',\hat{\mu}'), \tag{156}$$

$$\mathbf{T}^{\dagger}(\hat{\mu},\hat{\mu}') = \mathbf{T}_1^{\dagger}(\hat{\mu},\hat{\mu}')\mathbf{X}(\psi,\Psi,-\hat{\mu}') + \mathbf{X}(0,\psi,-\hat{\mu})\mathbf{D}^{\dagger}(\psi,\hat{\mu},\hat{\mu}') + \tfrac{1}{\pi}\int \mathrm{d}\hat{\mu}''\mu''\,\mathbf{T}_1^{\dagger}(\hat{\mu},\hat{\mu}'')\mathbf{D}^{\dagger}(\psi,\hat{\mu}'',\hat{\mu}'). \tag{157}$$

The interpretation of Eqs. (148)–(151) and (154)–(157) is clear. For example, Eq. (148) indicates that the upwelling radiation at the interface between layers 1 and 2 in response to the beam incident on the combined layer from above is simply the result of the reflection of the corresponding downwelling radiation by layer 2. This downwelling radiation consists of the attenuated direct component represented by the matrizant $\mathbf{X}(\psi,0,\hat{\mu}')$ (photon trajectory 1 in Fig. 20) and the diffuse component represented by the matrix $\mathbf{D}(\psi,\hat{\mu}'',\hat{\mu}')$ (photon trajectory 2 in Fig. 20). Similarly, Eq. (154) shows that the reflected radiation in response to the beam illuminating the combined layer from above consists of three components: (i) the photons that never reached the interface between layers 1 and 2 (the first term on the right-hand side of Eq. (154) and photon trajectory 1 in Fig. 21); (ii) the photons reflected by layer 2 and transmitted by layer 1 without scattering (the second term on the right-hand side of Eq. (154) and photon trajectory 2 in Fig. 21); and (iii) the photons reflected by layer 2 and diffusely transmitted by layer 1 (the third term on the right-hand side of Eq. (154) and photon trajectory 3 in Fig. 21). The reader may find it a useful exercise to give similar graphical interpretations of Eqs. (149)–(151) and (155)–(157).

Equations (148)–(151) and (154)–(157) are called adding equations because they allow one to compute the scattering properties of the combined layer provided that the scattering properties of each component layer are known. Indeed, if the matrices $\mathbf{R}_1$, $\mathbf{T}_1$, $\mathbf{R}_1^{\dagger}$, and $\mathbf{T}_1^{\dagger}$ for layer 1 in isolation from layer 2 and the matrices $\mathbf{R}_2$, $\mathbf{T}_2$, $\mathbf{R}_2^{\dagger}$, and $\mathbf{T}_2^{\dagger}$ for layer 2 in isolation from layer 1 are known then one can solve Eqs. (148)–(151) and find the

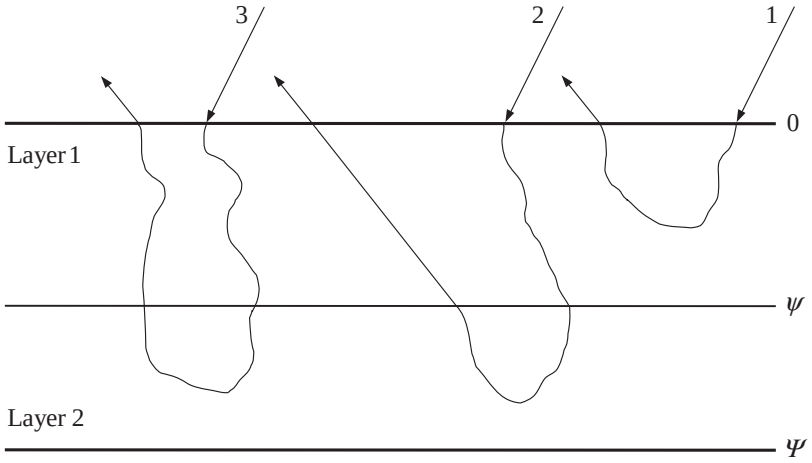

Fig. 21. Physical interpretation of Eq. (154).

matrices $\mathbf{D}$, $\mathbf{U}$, $\mathbf{D}^{\dagger}$, and $\mathbf{U}^{\dagger}$ describing the radiation field at the interface between the layers in the combined slab. This procedure involves replacing the angular integrals by appropriate quadrature sums. For example, Eq. (148) becomes

$$\mathbf{U}(\psi;\mu_i,\varphi_j;\mu_k,\varphi_l)=\mathbf{R}_2(\mu_i,\varphi_j;\mu_k,\varphi_l)\mathbf{X}(\psi,0;\mu_k,\varphi_l)$$
$$+\frac{1}{\pi}\sum_{m=1}^{N_\mu}\sum_{n=1}^{N_\varphi} w_m u_n \mu_m \mathbf{R}_2(\mu_i,\varphi_j;\mu_m,\varphi_n)\,\mathbf{D}(\psi;\mu_m,\varphi_n;\mu_k,\varphi_l),$$

where μ_i and w_i $(i=1,...,N_\mu)$ are quadrature division points and weights on the interval [0, 1] and φ_i and u_i $(i=1,...,N_\varphi)$ are quadrature division points and weights on the interval $[0,2\pi]$. The resulting system of linear algebraic equations for the unknown values of the matrices $\mathbf{D}$, $\mathbf{U}$, $\mathbf{D}^{\dagger}$, and $\mathbf{U}^{\dagger}$ at the quadrature division points can be solved using one of many available numerical techniques. After the matrices $\mathbf{D}$, $\mathbf{U}$, $\mathbf{D}^{\dagger}$, and $\mathbf{U}^{\dagger}$ at the quadrature division points are found, the reflection and transmission matrices of the combined layer can be calculated using the discretized version of Eqs. (154)–(157). Adding two identical layers is traditionally called the doubling procedure.

Furthermore, let us assume that the matrices $\mathbf{U}_1$, $\mathbf{D}_1$, $\mathbf{U}_1^{\dagger}$, and $\mathbf{D}_1^{\dagger}$ for a vertical level inside layer 1 are known, where the subscript 1 indicates that these matrices pertain to layer 1 taken in isolation from layer 2. Then the matrices $\mathbf{U}$, $\mathbf{D}$, $\mathbf{U}^{\dagger}$, and $\mathbf{D}^{\dagger}$ for the same level in the combined layer can also be easily calculated. Indeed, applying Eqs. (138) and (139) to each component layer and to the combined layer, we derive

$$\mathbf{U}(\psi',\hat{\mu},\hat{\mu}')=\mathbf{U}_1(\psi',\hat{\mu},\hat{\mu}')+\mathbf{X}(\psi',\psi,-\hat{\mu})\mathbf{U}(\psi,\hat{\mu},\hat{\mu}')$$
$$+\tfrac{1}{\pi}\int \mathrm{d}\hat{\mu}''\mu''\mathbf{D}_1^{\dagger}(\psi',\hat{\mu},\hat{\mu}'')\mathbf{U}(\psi,\hat{\mu}'',\hat{\mu}'), \qquad (158)$$

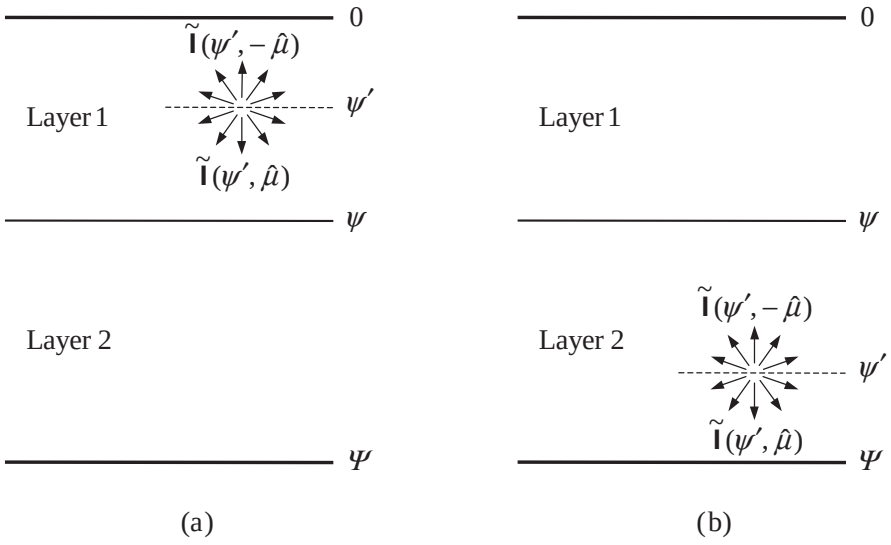

Fig. 22. Internal radiation field.

$$\mathbf{D}(\psi', \hat{\mu}, \hat{\mu}') = \mathbf{D}_1(\psi', \hat{\mu}, \hat{\mu}') + \tfrac{1}{\pi} \int \mathrm{d}\hat{\mu}'' \mu'' \mathbf{U}_1^{\dagger}(\psi', \hat{\mu}, \hat{\mu}'') \mathbf{U}(\psi, \hat{\mu}'', \hat{\mu}') , \tag{159}$$

$$\mathbf{U}^{\dagger}(\psi', \hat{\mu}, \hat{\mu}') = \mathbf{U}_1^{\dagger}(\psi', \hat{\mu}, \hat{\mu}') \mathbf{X}(\psi, \Psi, -\hat{\mu}') + \tfrac{1}{\pi} \int \mathrm{d}\hat{\mu}'' \mu'' \mathbf{U}_1^{\dagger}(\psi', \hat{\mu}, \hat{\mu}'') \mathbf{D}^{\dagger}(\psi, \hat{\mu}'', \hat{\mu}') , \tag{160}$$

$$\mathbf{D}^{\dagger}(\psi', \hat{\mu}, \hat{\mu}') = \mathbf{D}_1^{\dagger}(\psi', \hat{\mu}, \hat{\mu}') \mathbf{X}(\psi, \Psi, -\hat{\mu}') + \mathbf{X}(\psi', \psi, -\hat{\mu}) \mathbf{D}^{\dagger}(\psi, \hat{\mu}, \hat{\mu}') + \tfrac{1}{\pi} \int \mathrm{d}\hat{\mu}'' \mu'' \mathbf{D}_1^{\dagger}(\psi', \hat{\mu}, \hat{\mu}'') \mathbf{D}^{\dagger}(\psi, \hat{\mu}'', \hat{\mu}') \tag{161}$$

for $\psi' \in [0, \psi]$ (Fig. 22(a)). Similarly, if we know the matrices $\mathbf{U}_2$, $\mathbf{D}_2$, $\mathbf{U}_2^{\dagger}$, and $\mathbf{D}_2^{\dagger}$ for a vertical level inside layer 2 taken in isolation from layer 1 then

$$\mathbf{U}(\psi', \hat{\mu}, \hat{\mu}') = \mathbf{U}_2(\psi' - \psi, \hat{\mu}, \hat{\mu}') \mathbf{X}(\psi, 0, \hat{\mu}') + \tfrac{1}{\pi} \int \mathrm{d}\hat{\mu}'' \mu'' \mathbf{U}_2(\psi' - \psi, \hat{\mu}, \hat{\mu}'') \mathbf{D}(\psi, \hat{\mu}'', \hat{\mu}') , \tag{162}$$

$$\mathbf{D}(\psi', \hat{\mu}, \hat{\mu}') = \mathbf{D}_2(\psi' - \psi, \hat{\mu}, \hat{\mu}') \mathbf{X}(\psi, 0, \hat{\mu}') + \mathbf{X}(\psi', \psi, \hat{\mu}) \mathbf{D}(\psi, \hat{\mu}, \hat{\mu}') + \tfrac{1}{\pi} \int \mathrm{d}\hat{\mu}'' \mu'' \mathbf{D}_2(\psi' - \psi, \hat{\mu}, \hat{\mu}'') \mathbf{D}(\psi, \hat{\mu}'', \hat{\mu}') , \tag{163}$$

$$\mathbf{U}^{\dagger}(\psi', \hat{\mu}, \hat{\mu}') = \mathbf{U}_2^{\dagger}(\psi' - \psi, \hat{\mu}, \hat{\mu}') + \mathbf{X}(\psi', \psi, \hat{\mu}) \mathbf{U}^{\dagger}(\psi, \hat{\mu}, \hat{\mu}') + \tfrac{1}{\pi} \int \mathrm{d}\hat{\mu}'' \mu'' \mathbf{D}_2(\psi' - \psi, \hat{\mu}, \hat{\mu}'') \mathbf{U}^{\dagger}(\psi, \hat{\mu}'', \hat{\mu}') , \tag{164}$$

$$\mathbf{D}^{\dagger}(\psi', \hat{\mu}, \hat{\mu}') = \mathbf{D}_2^{\dagger}(\psi' - \psi, \hat{\mu}, \hat{\mu}') + \tfrac{1}{\pi} \int \mathrm{d}\hat{\mu}'' \mu'' \mathbf{U}_2(\psi' - \psi, \hat{\mu}, \hat{\mu}'') \mathbf{U}^{\dagger}(\psi, \hat{\mu}'', \hat{\mu}') \tag{165}$$

for $\psi' \in [\psi, \Psi]$ (Fig. 22(b)). The physical meaning of these formulas is rather transparent.

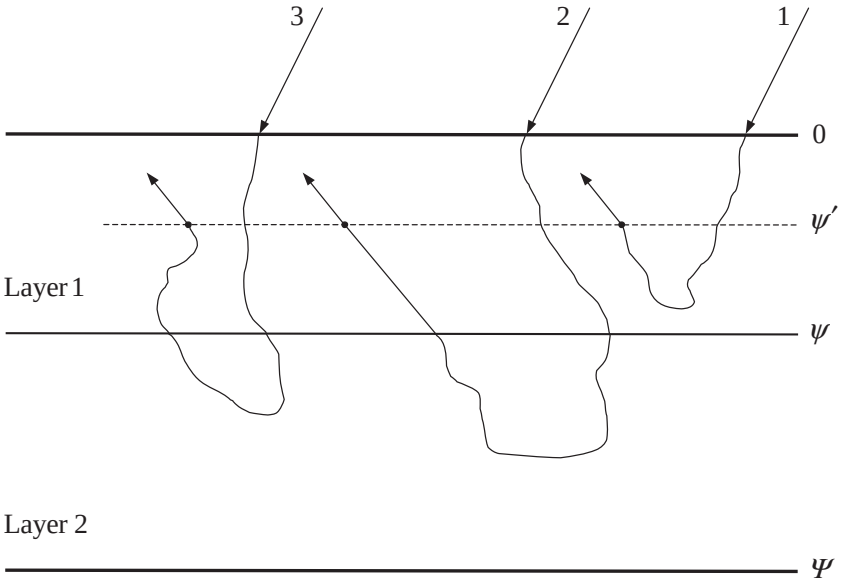

Fig. 23. Physical interpretation of Eq. (158).

For example, the first term on the right-hand side of Eq. (158) represents the contribution of photons that never reached the interface between layers 1 and 2, as shown schematically by photon trajectory 1 in Fig. 23. The second term describes the contribution of the photons that crossed the interface, exited layer 2 in the direction $\hat{\mu}$, and reached the level ψ' without scattering, as illustrated by photon trajectory 2 in Fig. 23. The last term gives the contribution of the photons that crossed the interface and were scattered at least once inside layer 1 before they reached the level ψ' (trajectory 3 in Fig. 23).

A practical implementation of the adding method can involve the following basic steps.

(1) A vertically inhomogeneous layer of particle thickness Ψ is approximated by a stack of N partial homogeneous layers having particle thicknesses $\Psi_1, ..., \Psi_N$ such that $\Psi = \sum_{n=1}^{N} \Psi_n$ (Fig. 24). The number of partial layers and their partial thicknesses can depend on the degree of vertical inhomogeneity of the original layer as well as on the desired numerical accuracy of computations.

(2) The reflection and transmission matrices $\mathbf{R}_n, \mathbf{T}_n, \mathbf{R}_n^{\dagger}$, and $\mathbf{T}_n^{\dagger}$ of partial layer n in isolation from all other layers are computed by using the doubling method (Fig. 25). The doubling process can be started with a layer having a particle thickness $\Delta\Psi_n = \Psi_n / 2^{k_n}$ small enough that the reflection and transmission matrices for this layer can be computed by considering only the first order of scattering. Specifically, choosing the number of doubling events k_n sufficiently large that all elements of the matrices $\Delta\Psi_n \mathbf{Z}_n$ and $\Delta\Psi_n \mathbf{K}_n$ are much smaller than unity, using Eqs. (117) and (136)–(143), and neglecting all terms proportional to $(\Delta\Psi_n)^m$ with $m > 1$, we derive

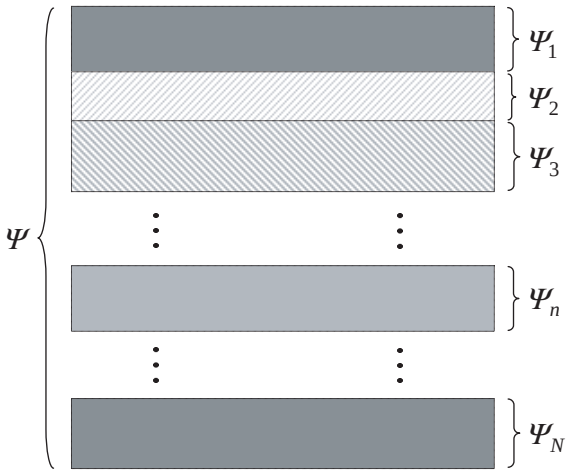

Fig. 24. Representation of a vertically inhomogeneous scattering layer by a stack of N homogeneous sublayers.

$$\mathbf{X}_n(\Delta\Psi_n, 0, \hat{\mu}') = \mathbf{\Delta} - \frac{\Delta\Psi_n}{\mu'}\mathbf{K}_n(\hat{\mu}'), \tag{166}$$

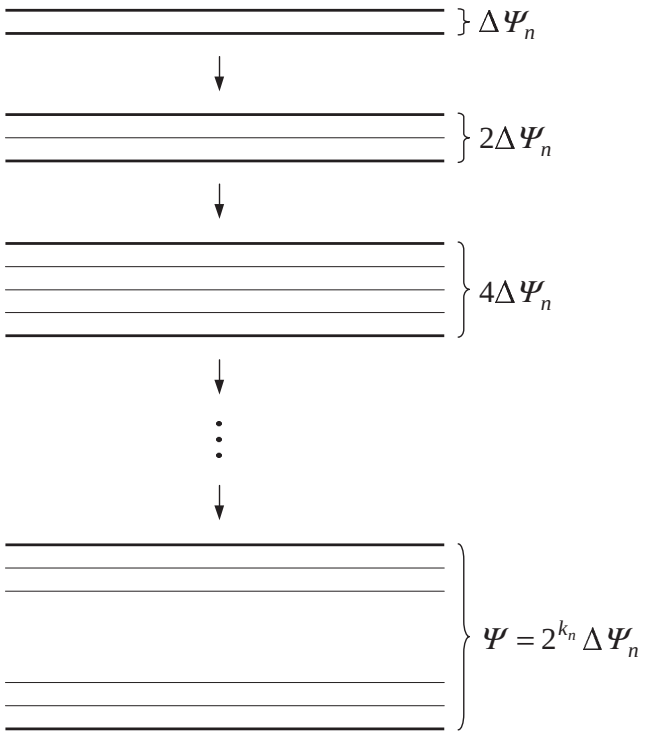

Fig. 25. The doubling procedure.

$$\mathbf{X}_n(0, \Delta\Psi_n, -\hat{\mu}) = \mathbf{\Delta} - \frac{\Delta\Psi_n}{\mu}\mathbf{K}_n(-\hat{\mu}) . \tag{167}$$

$$\mathbf{R}_n(\hat{\mu}, \hat{\mu}') = \frac{\pi\Delta\Psi_n}{\mu\mu'}\mathbf{Z}_n(-\hat{\mu}, \hat{\mu}') , \tag{168}$$

$$\mathbf{T}_n(\hat{\mu}, \hat{\mu}') = \frac{\pi\Delta\Psi_n}{\mu\mu'}\mathbf{Z}_n(\hat{\mu}, \hat{\mu}') , \tag{169}$$

$$\mathbf{R}_n^{\dagger}(\hat{\mu}, \hat{\mu}') = \frac{\pi\Delta\Psi_n}{\mu\mu'}\mathbf{Z}_n(\hat{\mu}, -\hat{\mu}') , \tag{170}$$

$$\mathbf{T}_n^{\dagger}(\hat{\mu}, \hat{\mu}') = \frac{\pi\Delta\Psi_n}{\mu\mu'}\mathbf{Z}_n(-\hat{\mu}, -\hat{\mu}') , \tag{171}$$

Obviously, the doubling procedure will also yield the matrices $\mathbf{U}_n$, $\mathbf{D}_n$, $\mathbf{U}_n^{\dagger}$, and $\mathbf{D}_n^{\dagger}$ at $2^{k_n} - 1$ equidistant levels inside the *n*th partial layer (Fig. 25).

(3) The *N* partial homogeneous layers are recursively added starting from layer 1 and moving down or starting from layer *N* and moving up. This process gives the reflection and transmission matrices of the combined slab and the matrices $\mathbf{U}$, $\mathbf{D}$, $\mathbf{U}^{\dagger}$, and $\mathbf{D}^{\dagger}$ at the $N - 1$ interfaces between the partial layers as well as at the $\sum_{n=1}^{N}(2^{k_n} - 1)$ levels inside the partial layers rendered by the doubling procedure.

Numerical solution of the adding equations requires the knowledge of the ensemble-averaged extinction and phase matrices. The exact and approximate theoretical methods applicable to single-scattering computations for small particles have been extensively reviewed in recent books by Mishchenko *et al.* [26, 31] and will not be specifically discussed here. Those books also provide a detailed discussion of extinction, scattering, and absorption properties of particles having diverse morphologies and compositions and encountered in various environments.

The adding concept goes back to Stokes [32], who analyzed the reflection and transmission of light by a stack of glass plates, and was introduced to radiative transfer by van de Hulst [33]. Our derivation of the adding equations for scattering layers consisting of arbitrarily oriented nonspherical particles largely follows [34].

The adding equations become significantly simpler for macroscopically isotropic and mirror-symmetric scattering media (cf. Eq. (110)). A definitive account of this situation can be found in [35, 36]. Multiple remote sensing and astrophysical applications of the RTT can be found in [6–11, 13, 15, 31, 37–40].

5. Acknowledgments

We thank Yuri Barabanenkov, Joop Hovenier, Michael Kahnert, Andrew Lacis, Larry Travis, Cornelis van der Mee, and Edgard Yanovitskii for many fruitful discussions. This research was funded by the NASA Radiation Sciences Program managed by Donald Anderson.

References

1. O. D. Khvolson, Grundzüge einer mathematischen Theorie der inneren Diffusion des Lichtes, *Bull. St. Petersburg Acad. Sci.* **33**, 221–256 (1890).
2. A. Schuster, Radiation through a foggy atmosphere, *Astrophys. J.* **21**, 1–22 (1905).
3. J. E. Hansen and L. D. Travis, Light scattering in planetary atmospheres, *Space. Sci. Rev*. **16**, 527–610 (1974).
4. J. W. Hovenier and C. V. M. van der Mee, Fundamental relationships relevant to the transfer of polarized light in a scattering atmosphere, *Astron. Astrophys*. **128**, 1–16 (1983).
5. J. Lenoble, ed., *Radiative Transfer in Scattering and Absorbing Atmospheres* (A. Deepak, Hampton, Va., 1985).
6. A. K. Fung, *Microwave Scattering and Emission Models and Their Applications* (Artech House, Boston, 1994).
7. A. Z. Dolginov, Yu. N. Gnedin, and N. A. Silant'ev, *Propagation and Polarization of Radiation in Cosmic Media* (Gordon and Breach, Basel,1995).
8. E. G. Yanovitskij, *Light Scattering in Inhomogeneous Atmospheres* (Springer, Berlin, 1997).
9. G. E. Thomas and K. Stamnes, *Radiative Transfer in the Atmosphere and Ocean* (Cambridge Univ. Press, New York, 1999).
10. K. N. Liou, *An Introduction to Atmospheric Radiation* (Academic Press, San Diego, 2002).
11. J. W. Hovenier, C. V. M. van der Mee, and H. Domke, *Transfer of Polarized Light in Planetary Atmospheres* (Kluwer, Dordrecht, 2003).
12. V. Kourganoff, *Basic Methods in Transfer Problems* (Clarendon, Oxford, 1952).
13. S. Chandrasekhar, *Radiative Transfer* (Dover, New York, 1960).
14. V. V. Sobolev, *Light Scattering in Planetary Atmospheres* (Pergamon, Oxford, 1974).
15. H. C. van de Hulst, *Multiple Light Scattering* (Academic Press, New York, 1980).
16. L. Mandel and E. Wolf, *Optical Coherence and Quantum Optics* (Cambridge University Press, Cambridge, 1995).
17. A. G. Borovoy, Method of iterations in multiple scattering: the transfer equation, *Izv. Vuzov. Fizika*, No. 6, 50–54 (1966).
18. Yu. N. Barabanenkov and V. M. Finkel'berg, Radiation transport equation for correlated scatterers, *Soviet Phys. JETP* **26**, 587–591 (1968).
19. A. Z. Dolginov, Yu. N. Gnedin, and N. A. Silant'ev, Photon polarization and frequency change in multiple scattering, *J. Quant. Spectrosc. Radiat. Transfer* **10**, 707–754 (1970).
20. L. A. Apresyan and Yu. A. Kravtsov, *Radiation Transfer* (Gordon and Breach, Basel, 1996).
21. A. Lagendijk and B. A. van Tiggelen, Resonant multiple scattering of light, *Phys. Rep.* **270**, 143–215 (1996).
22. A. Ishimaru, *Wave Propagation and Scattering in Random Media* (IEEE Press, New York, 1997).
23. L. Tsang and J. A. Kong, *Scattering of Electromagnetic Waves: Advanced Topics* (Wiley, New York, 2001).
24. V. P. Tishkovets, Multiple scattering of light by a layer of discrete random medium: backscattering, *J. Quant. Spectrosc. Radiat. Transfer* **72**, 123–137 (2002).
25. M. I. Mishchenko, Vector radiative transfer equation for arbitrarily shaped and arbitrarily oriented particles: a microphysical derivation from statistical electromagnetics, *Appl. Opt*. **41**, (2002).
26. M. I. Mishchenko, L. D. Travis, and A. A. Lacis, *Scattering, Absorption, and Emission of Light by Small Particles* (Cambridge University Press, Cambridge, 2002).
27. V. Twersky, On propagation in random media of discrete scatterers, *Proc. Symp. Appl. Math.* **16**, 84–116 (1964).
28. D. S. Saxon, Lectures on the scattering of light (Science Report No. 9, Department of Meteorology, University of California, Los Angeles, 1955).
29. M. I. Mishchenko, A. A. Lacis, and L. D. Travis, Errors introduced by the neglect of

polarization in radiance calculations for Rayleigh-scattering atmospheres, *J. Quant. Spectrosc. Radiat. Transfer* **51**, 491–510 (1994).

30. J. E. Hansen, Multiple scattering of polarized light in planetary atmospheres. II. Sunlight reflected by terrestrial water clouds, *J. Atmos. Sci.* **28**, 1400–1426 (1971).
31. M. I. Mishchenko, J. W. Hovenier, and L. D. Travis, L. D., eds., *Light Scattering by Nonspherical Particles: Theory, Measurements, and Applications* (Academic Press, San Diego, 2000).
32. G. G. Stokes, On the intensity of the light reflected from or transmitted through a pile of plates, *Proc. R. Soc. London* **11**, 545–556 (1862).
33. H. C. van de Hulst, A new look at multiple scattering (Technical Report, NASA Institute for Space Studies, New York, 1963).
34. M. I. Mishchenko, Multiple scattering of light in anisotropic plane-parallel media, *Transp. Theory Stat. Phys*. **19**, 293–316 (1990).
35. J. F. de Haan, P. B. Bosma, and J. W. Hovenier, The adding method for multiple scattering calculations of polarized light, *Astron. Astrophys.* **183**, 371–391 (1987).
36. P. Stammes, J. F. de Haan, and J. W. Hovenier, The polarized internal radiation field of a planetary atmosphere, *Astron. Astrophys.* **225**, 239–259 (1989).
37. G. Asrar, ed., *Theory and Applications of Optical Remote Sensing* (John Wiley, New York, 1989).
38. G. L. Stephens, *Remote Sensing of the Lower Atmosphere* (Oxford University Press, New York, 1994).
39. C. D. Mobley, *Light and Water: Radiative Transfer in Natural Waters* (Academic Press, San Diego, 1994).
40. M. Mishchenko, J. Penner, and D. Anderson, eds., Special issue on Global Aerosol Climatology Project, *J. Atmos. Sci.* **59**, 249–783.